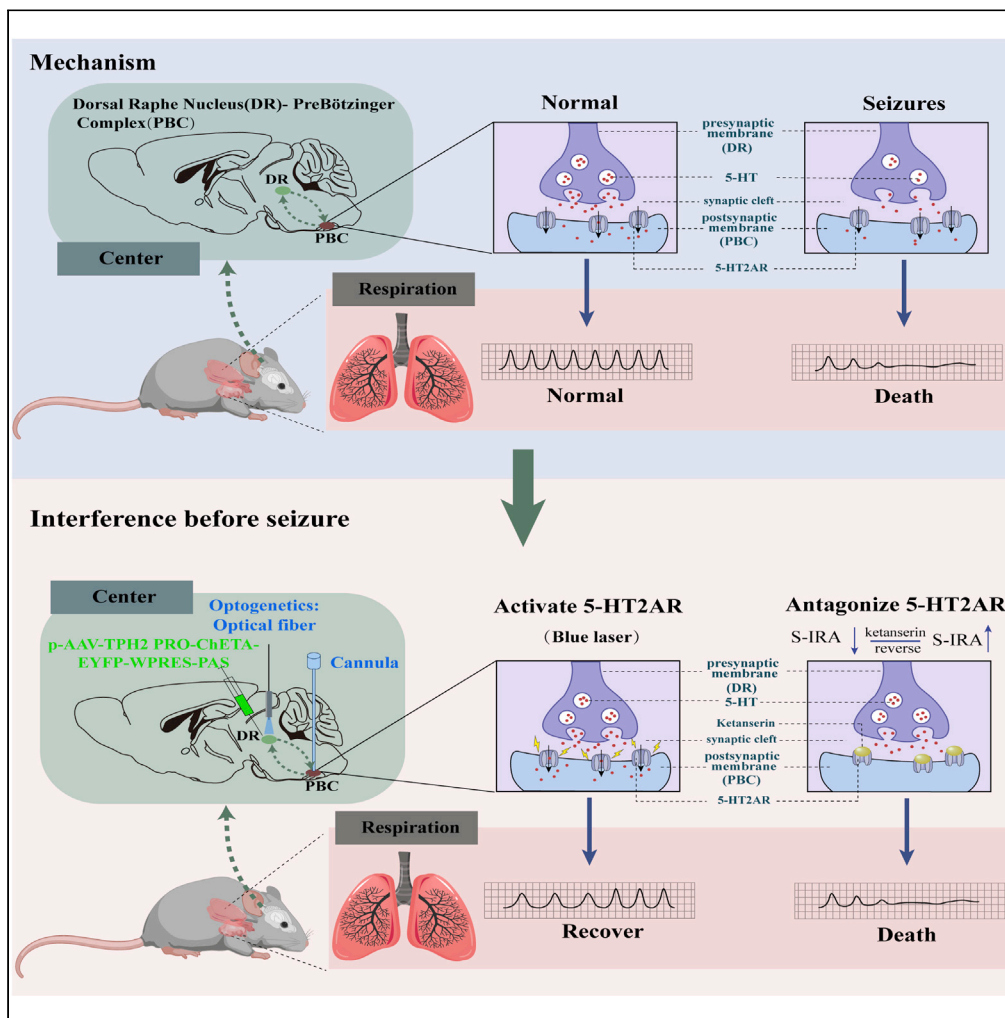


Article

Dorsal raphe nucleus to pre-Bötzinger complex serotonergic neural circuit is involved in seizure-induced respiratory arrest



HaiXiang Ma, Qian Yu, Yue Shen, ..., Chang Zeng, Kazuki Nagayasu, HongHai Zhang

zhanghonghai_0902@163.com

Highlights

The decreased incidence of S-IRA achieved by the administration of 5-HTP can be significantly reversed by ketanserin (KET), a selective antagonist of 5-HT_{2R} including A, B and C receptors

The serotonergic neural circuit between the DR and PBC is involved in modulating S-IRA

The suppressive effects of the optogenetic activation of the serotonergic neural circuit between the DR and PBC on S-IRA were obviously reversed by KET

The neural circuit between the DR and PBC and 5-HT_{2A}R in the PBC may be a specific and key target for preventing SUDEP

Ma et al., iScience 25, 105228
October 21, 2022 © 2022 The Author(s).
<https://doi.org/10.1016/j.isci.2022.105228>



Article

Dorsal raphe nucleus to pre-Bötzing complex serotonergic neural circuit is involved in seizure-induced respiratory arrest

HaiXiang Ma,^{1,2,9} Qian Yu,^{1,2,9} Yue Shen,^{1,2,3,9} XiTing Lian,^{1,9} LeYuan Gu,^{1,2} YuLing Wang,² Qing Xu,¹ Han Lu,⁵ HaiTing Zhao,⁶ Chang Zeng,⁷ Kazuki Nagayasu,⁸ and HongHai Zhang^{1,2,3,4,10,*}

SUMMARY

Sudden unexpected death in epilepsy (SUDEP) is the leading cause of death among patients with epilepsy. However, the underlying mechanism of SUDEP remains elusive. Previous studies showed seizure-induced respiratory arrest (S-IRA) is the main factor in SUDEP, and that enhancement of serotonin (5-HT) function in the dorsal raphe nucleus (DR) can significantly reduce the incidence of S-IRA in the DBA/1 mouse model of SUDEP. The pre-Bötzing complex (PBC), known for its role in regulating respiratory rhythm, can express the 5-HT_{2A} receptor (5-HT_{2AR}). Here, using the pharmacological and optogenetic methods, respectively, we observed that the serotonergic neural circuit between DR and PBC was involved in S-IRA evoked by either acoustic stimulation or pentylenetetrazole (PTZ) injection in the DBA/1 mice, and found 5-HT_{2AR} located in PBC plays an important role in it. Our findings will further significantly improve our understanding of SUDEP and provide a promising therapeutic target for SUDEP prevention.

INTRODUCTION

Continuing research has demonstrated that sudden unexpected death in epilepsy (SUDEP) is the leading cause of death among patients with epilepsy, occurring even more frequently among patients with anti-epileptic drug resistance (Devinsky et al., 2016; Lhatoo et al., 2015; Massey et al., 2014; Ryvlin et al., 2013). Currently, respiratory dysfunction during seizures is considered to be the main mechanism of SUDEP. The latest advancements in the pathogenesis of SUDEP revealed that cardiopulmonary dysfunction might also play an important role in the occurrence of SUDEP (Devinsky et al., 2016; Lhatoo et al., 2015; Massey et al., 2014; Ryvlin et al., 2013; Vilella et al., 2019). Some studies have indicated that several selective serotonin (5-HT) reuptake inhibitors (SSRIs) can prevent seizure-induced respiratory arrest (S-IRA) evoked by generalized audiogenic seizures (AGSz) in DBA/1 mice by elevating the 5-HT level in the synaptic cleft (Bateman et al., 2010a; Buchanan et al., 2014; Ozawa and Okado, 2002). However, owing to the limitations of SUDEP animal models, the role of 5-HT synthesis and the specific effects of targeting 5-HT receptors in the brain in modulating S-IRA and SUDEP remain unclear.

It had been accepted that tryptophan hydroxylase-2 (TPH2) in the brain could convert L-tryptophan to 5-hydroxytryptophan (5-HTP), which could be further converted to 5-HT by aromatic L-amino acid decarboxylase (Donato Di Paola et al., 2007; Kulikov et al., 2005; Osipova et al., 2010). A previous study showed that TPH2 existed in the brain as the rate-limiting enzyme in 5-HT synthesis (Kulikov et al., 2005, p. 2). Our group previously tested the correlation between the content of TPH2 protein expression and activity and found that TPH2 protein expression varied consistently with TPH2 activity, and within the same model, we found that TPH2 protein expression varied consistently with TPH2 activity (Zeng et al., 2015). Thus, the expression of TPH2 is vital for the conversion of endogenous 5-HTP to 5-HT, which is necessary for reducing the incidence of S-IRA and preventing SUDEP. However, how 5-HT mediates both S-IRA and the SUDEP in our mouse model remains unclear.

Our previous research showed that S-IRA could lead to the occurrence of SUDEP evoked by either acoustic stimulation or pentylenetetrazole (PTZ) injection in a DBA/1 mouse model (Chen et al., 2019; Vilella et al., 2019; Zeng et al., 2015; Zhang et al., 2016, 2017; Zhao et al., 2017, 2019), and the incidence of S-IRA evoked

¹Department of Anesthesiology, Affiliated Hangzhou First People's Hospital, Zhejiang University School of Medicine, Hangzhou 310006, China

²Department of Anesthesiology, the Fourth Clinical School of Medicine, Zhejiang Chinese Medical University, Hangzhou 310006, China

³Department of Anesthesiology, Hangzhou First People's Hospital, Nanjing Medical University, Hangzhou 310006, China

⁴Westlake Laboratory of Life Sciences and Biomedicine, Hangzhou 310006, China

⁵Department of Anesthesiology, Ruijin Hospital, Shanghai Jiao Tong University School of Medicine, Shanghai, China

⁶Department of Neurology, Xiangya Hospital, Central South University, Changsha 410008, China

⁷Health Management Center, Xiangya Hospital, Central South University, Changsha 410008

⁸Department of Molecular Pharmacology, Graduate School of Pharmaceutical Sciences, Kyoto University, Kyoto, Japan

⁹These authors contributed equally

¹⁰Lead contact

*Correspondence: zhanghonghai_0902@163.com

<https://doi.org/10.1016/j.isci.2022.105228>



by acoustic stimulation or PTZ treatment was significantly reduced by the treatment of 5-HTP in two models (Vilella et al., 2019). Studies have shown that the primary cause of death in epileptic mice is respiratory failure. Mechanical ventilation during the seizure or 5-HT_{2A}R agonist pretreatment can reduce the mortality rate of mice (Buchanan et al., 2014). Therefore, we hypothesized that 5-HT_{2A}R might play a crucial role in SUDEP. However, the key target within the brain that mediates the 5-HTP-induced reduction in S-IRA and SUDEP has not yet been identified. Considering the evidence that 5-HT_{2A}R is a key factor mediating respiratory function in the brainstem (Nagai et al., 2020; Tryba et al., 2006), we questioned whether the application of 5-HTP could reduce the incidence of S-IRA by targeting 5-HT_{2A}R in certain brain regions. Given that a previous study showed that the activation of 5-HT_{2B/2C}R by its agonist had no effects on the S-IRA in DBA/1 SUDEP models (Faingold et al., 2011), we chose the ketanserin (KET), a selective antagonist of 5-HT_{2A}R including 5-HT_{2A}, B and C receptors, to specifically target 5-HT_{2A}R to test its role in our models, and we hypothesized that the suppressive effects of 5-HTP against S-IRA could be reversed by KET aiming at 5-HT_{2A}R in our models, offering 5-HT_{2A}R a potential therapeutic target for preventing SUDEP.

To investigate the roles of 5-HTP and 5-HT_{2A}R in the pathogenesis of S-IRA and SUDEP, we continued to apply acoustic stimulation and PTZ injection in the DBA/1 mouse SUDEP model to test the ability of KET to reverse the effects of 5-HTP observed in our previous study.

The pre-Bötzinger complex (PBC) plays a necessary role in the generation of a normal relaxed respiratory rhythm. The PBC is located ventral to the caudal end of the compact part of the nucleus ambiguus, within the ventral respiratory column of the ventrolateral medulla (Alheid et al., 2002). In slice preparation at the level of PBC, the burst frequency of hypoglossal neurons in the inspiratory phase was increased by the application of 5-HT, suggesting that 5-HT excites the PBC neurons and increases the respiratory frequency (Ptak et al., 2009).

Considering the localization of 5-HT_{2A}R in the PBC, which plays a key role in regulating respiratory rhythm, we subsequently examined whether KET acted on 5-HT_{2A}R in the PBC (Chen et al., 2019). 5-HTergic neurons are mainly distributed in various subregions of the raphe nuclei that are distributed near the midline of the brainstem (Ren et al., 2019). The dorsal raphe (DR) is the predominant source of 5-HT innervation of the forebrain and is involved in a variety of functions, including anxiety, depression, and sleep-wake cycles, especially increased respiration and arousal induced by elevated levels of CO₂, which are often impaired by seizures contributing to S-IRA (Andalman et al., 2019; Kawashima et al., 2016). Studies have shown that the activity of 5-HT neurons in DR is closely related to epilepsy, and inhibition of hyperactivity of DR 5-HTergic neurons may present a promising anti-seizure effect (Cheng et al., 2021). In addition, physiological studies reported that electrical and chemical stimulation of both rostral and caudal raphe nuclei, including DR, changed respiratory patterns and serotonergic neurons in raphe nuclei projected throughout the VRC (ventral respiratory column), especially PBC (Morinaga et al., 2019). We hypothesized that the change in respiration pattern might be related to PBC by 5-HT. To test this hypothesis, we activate the neural circuit between DR and PBC using optogenetics technology. Based on our previous finding that S-IRA in DBA/1 mice could be significantly prevented by the optogenetic activation of TPH2-Channelrhodopsin 2 (ChR2) neurons in the DR, we further activated TPH2-ChETA neurons in the DR of DBA/1 mice to observe whether the suppression of S-IRA by the photostimulation of the DR in the PTZ injection model depended on the activation of 5-HT_{2A}R located in the PBC. Our findings indicate that the lower incidence of PTZ-induced S-IRA upon the optogenetic activation of TPH2-ChETA neurons in the DR was remarkably reversed by the injection of KET into the PBC. Meanwhile, it was confirmed that there was a neural circuit between the DR and PBC by injecting the tracer CTB-555 into DR and PBC, separately. Thus, our findings suggest that activating the neural circuit between the DR and the PBC might contribute to preventing SUDEP.

RESULTS

5-hydroxytryptophan-mediated suppression of seizure-induced respiratory arrest evoked by acoustic stimulation was reversed by IP injection of ketanserin

Compared with the vehicle group in primed DBA/1 mice, the incidence of S-IRA evoked by acoustic stimulation was significantly reduced after IP delivery of 5-HTP at a dosage of 200 mg/kg ($p < 0.001$). Moreover, compared with the vehicle group, the incidence of S-IRA in the group pretreated with 5-HTP (200 mg/kg, IP) and KET (5, 10, or 25 mg/kg, IP) was significantly decreased ($p < 0.01$, $p < 0.01$, $p < 0.05$), indicating that these dosages of KET did not significantly reverse the prohibitive effect of 5-HTP. However, the incidence

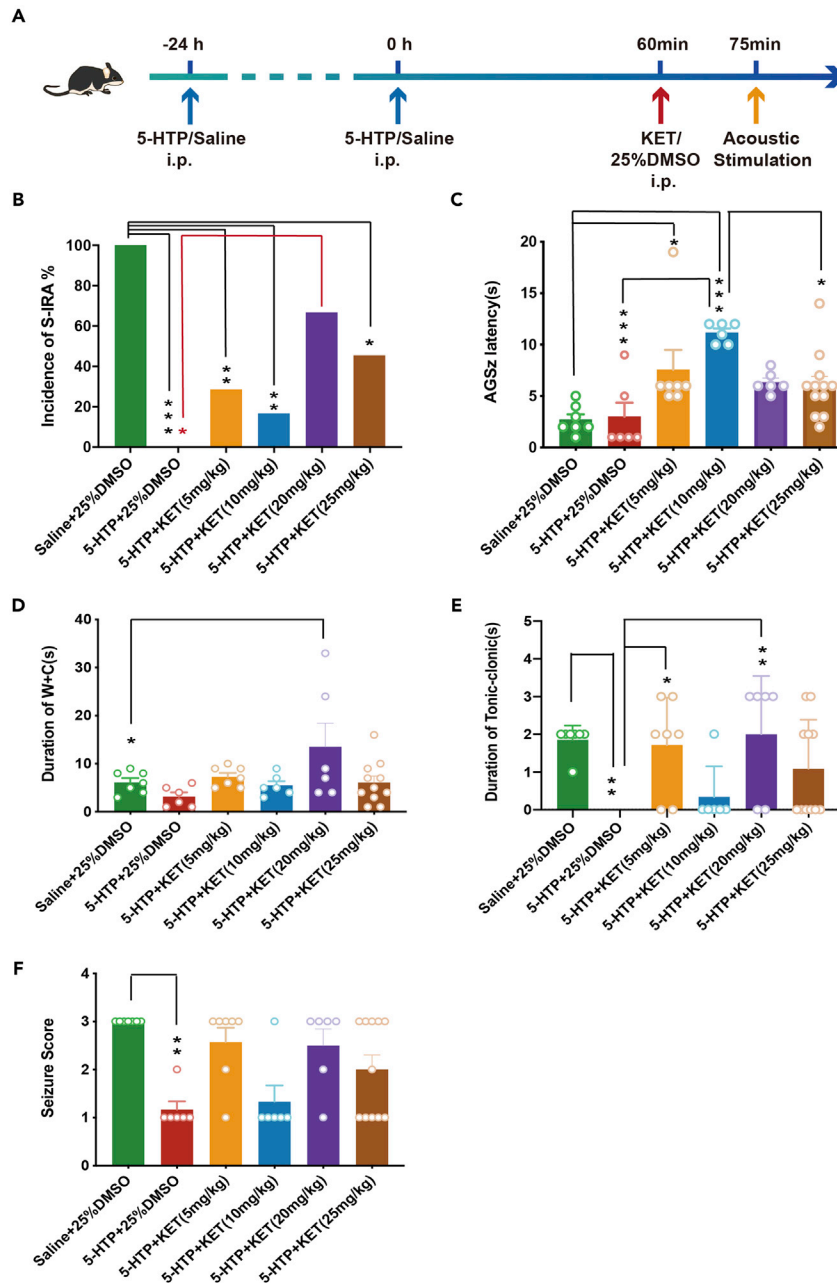


Figure 1. 5-HTP-mediated reduction in S-IRA evoked by acoustic stimulation was significantly reversed by the IP injection of KET

(A) Schematic illustration of the observation of changing of S-IRA in the DBA/1 mice by acoustic stimulation following IP of 5-HTP.

(B) Compared with that in the group treated with saline and 25% DMSO, the incidence of S-IRA evoked by acoustic stimulation was markedly lower in groups treated with 5-HTP and 25% DMSO ($n = 7$ and $n = 6$, respectively; $p < 0.001$). Compared to that in the control group treated with vehicle, the incidence of S-IRA was significantly reduced in the group treated with 5-HTP and KET (5, 10 mg/kg) ($n = 7$ and $n = 6$, respectively; $p < 0.01$). However, no difference was found between the control group and the group treated with 5-HTP and KET (20 mg/kg) ($n = 7$ and $n = 6$, respectively; $p > 0.05$). Furthermore, compared with the group treated with 5-HTP and 25% DMSO, the incidence of S-IRA in the group treated with 5-HTP and KET (20 mg/kg) was significantly increased ($n = 7$ and $n = 6$, respectively; $p < 0.05$). However, compared with the group treated with 5-HTP and 25% DMSO, the incidence of S-IRA in the group treated with 5-HTP and KET (25 mg/kg) was not significantly increased ($n = 7$ and $n = 11$, respectively; $p > 0.05$).

Figure 1. Continued

(C) Compared with the group pretreated with 5-HTP and KET (10 mg/kg), the latency to AGS_z was significantly reduced in the group 5-HTP + KET (25 mg/kg) ($p < 0.05$), 5-HTP + 25% DMSO ($p < 0.01$) and Vehicle +25% DMSO ($p < 0.01$).

(D) Compared with the vehicle group, duration of wild running plus clonic seizures (W + C) was remarkably increased in the group 5-HTP + KET (20 mg/kg) ($p < 0.05$).

(E) Duration of tonic-clonic seizures was significantly increased in the vehicle group ($p < 0.01$), 5-HTP + KET (5 mg/kg) ($p < 0.05$), and 5-HTP + KET (20 mg/kg) ($p < 0.01$) as compared with the group pretreated with 5-HTP and vehicle.

(F) Compared with the control group, the group treated with 5-HTP and vehicle was remarkably reduced in seizure score ($p < 0.05$).

of S-IRA showed no difference between the vehicle group and the group treated with 5-HTP (200 mg/kg, IP) and KET (20 mg/kg, IP; $p > 0.05$) and was significantly lower in the group treated with 5-HTP + 25% DMSO than in the group treated with KET (20 mg/kg, IP; $p < 0.05$). Thus, the suppressive effect of 5-HTP against S-IRA was markedly reversed by IP administration of 20 mg/kg KET (Figure 1B). Compared with the group pretreated with 5-HTP and KET (10 mg/kg), the latency to AGS_z was significantly reduced in the group 5-HTP + KET (25 mg/kg, $p < 0.05$), 5-HTP + 25%DMSO ($p < 0.01$) and Vehicle +25%DMSO ($p < 0.01$) (Figure 1C). Compared with the vehicle group, the duration of wild running plus clonic seizures (W + C) was remarkably increased in the group 5-HTP + KET (20 mg/kg, $p < 0.05$) (Figure 1D). The duration of tonic-clonic seizures was significantly increased in the vehicle group ($p < 0.01$), 5-HTP + KET (5 mg/kg, $p < 0.05$), and 5-HTP + KET (20 mg/kg, $p < 0.01$) as compared with the group pretreated with 5-HTP and vehicle (Figure 1E). The seizure scores were significantly lower in the group treated with 5-HTP and vehicle compared to the control group ($p < 0.05$) (Figure 1F). These findings regarding 5-HTP-mediated suppression of S-IRA evoked by acoustic stimulation were reversed by IP injection of KET.

5-hydroxytryptophan-mediated suppression of pentylenetetrazole-induced seizure-induced respiratory arrest was reversed by intracerebroventricular delivery of ketanserin

Compared with the vehicle control group, the incidence of PTZ-induced S-IRA was significantly reduced in the group that received ICV injection of 5-HTP and 25% DMSO ($p < 0.01$). Also, the incidence of PTZ-induced S-IRA was not significantly less in the group treated with 5-HTP and KET (9.15 nmol, ICV) compared with the vehicle group ($p > 0.05$). The incidence of PTZ-induced S-IRA was significantly higher in the group treated with 5-HTP and KET (18.30 nmol, ICV) than in the group treated with 5-HTP and 25% DMSO (ICV, $p < 0.05$), which suggested that the suppressive effect of 5-HTP against S-IRA was significantly reversed by KET at the ICV dosage of 18.30 nmol. Furthermore, compared with the vehicle control group, the incidence of PTZ-induced S-IRA in the group treated with 5-HTP + KET (18.30 nmol, ICV) was not significantly reduced ($p > 0.05$). Compared with the vehicle group, the duration of wild running plus clonic seizures (W + C) was remarkably reduced in the group 5-HTP + 25% DMSO ($p < 0.05$). The seizure scores from different groups did not differ significantly ($p > 0.05$), and no obvious influence on seizure behavior was observed within the reversal effects of KET (Figure 2).

ChETA expression was induced in the membrane of 5-HT neurons in the dorsal raphe nucleus of DBA/1 mice

The viral vector pAAV-TPH2 PRO-ChETA-EYFP-WPRES-PAS, under the control of the TPH2 promoter, was delivered into the DR of 50-day-old wild-type DBA/1 mice to create TPH2-ChETA-expressing mice. After 3 weeks, we first examined the expression of ChETA and TPH2 in 5-HT neurons in the DR of DBA/1 mice using immunohistochemistry ($n = 3$). The expression of EYFP, a surrogate marker for ChETA, was predominantly localized in the membranes of the cell body and axons of 5-HT neurons of the DR. TPH2 was predominantly confined to the cytosol of 5-HT neurons in the DR of DBA/1 mice. The ratio for merged expression of ChETA and TPH2 was 82.10%, which was approximately consistent with our previous work (Zhao et al., 2019) (Figures 3 and 4).

Activation of 5-HT neurons in the DR reduced PTZ-induced S-IRA in DBA/1 mice and the lower incidence of S-IRA by photostimulating the DR was significantly reversed by ICV delivery of KET.

We examined the effect of the selective enhancement of 5-HT neurotransmission on PTZ-induced S-IRA by applying photostimulation (blue light, 20-ms pulse duration, 20 Hz, 20 min) to 5-HT neurons in the DR of non-primed DBA/1 mice. Compared with the incidence of PTZ-induced S-IRA in DBA/1 mice without photostimulation ($n = 7$), after the photostimulation of the DR for 20 min was significantly decreased ($n = 6$, $p < 0.05$). However, after ICV administration of KET (18.30 nmol, ICV), the incidence of PTZ-induced

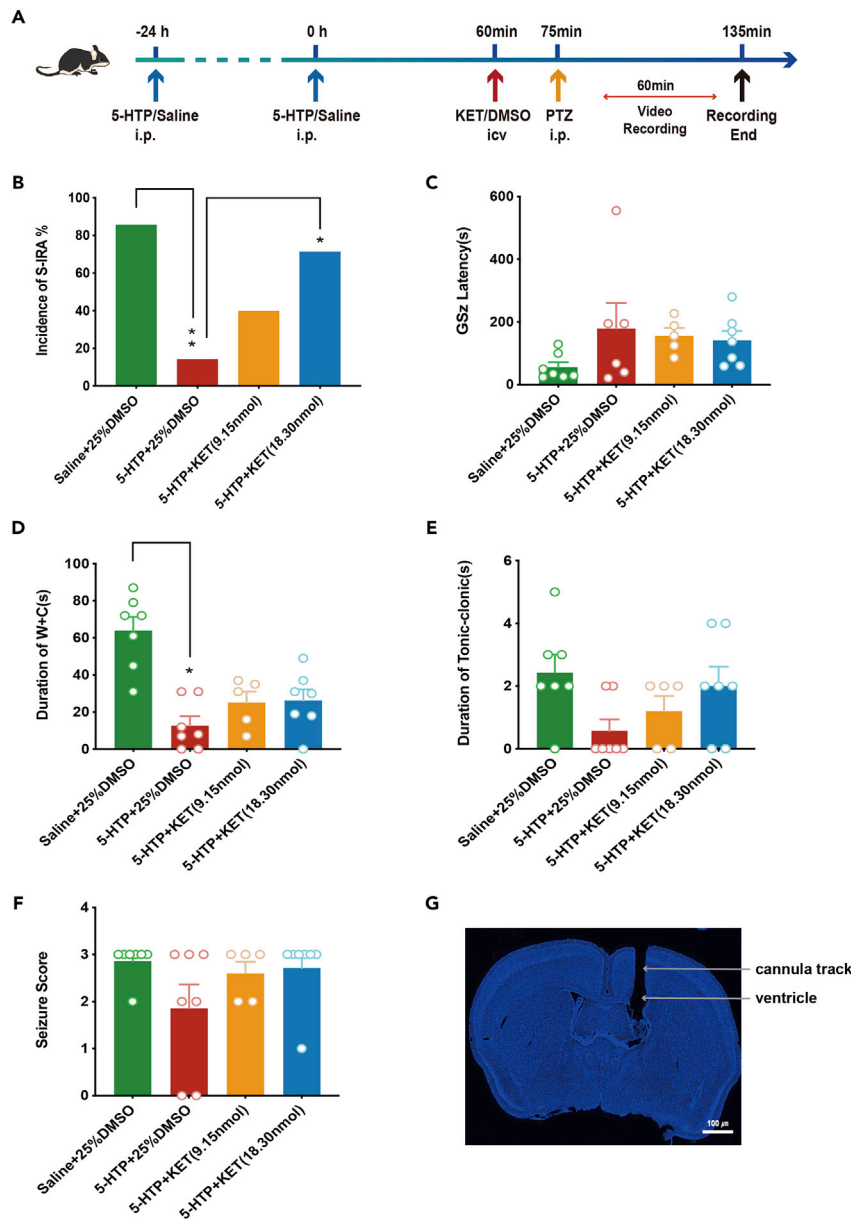


Figure 2. 5-HTP-mediated reduction in PTZ-induced S-IRA was significantly reversed by the ICV injection of KET

(A) Schematic illustration of the observation of changing of S-IRA in the DBA/1 mice by IP PTZ following IP of 5-HTP and ICV of KET.

(B) Compared to the control group, the incidence of PTZ-induced S-IRA was markedly lower in the group treated with 5-HTP and 25% DMSO ($p < 0.01$). However, no difference was observed between the control group and the groups treated with 5-HTP and KET (9.15 and 18.30 nmol; $p > 0.05$). By contrast, the incidence of S-IRA was significantly reduced in the group treated with 5-HTP and ICV 25% DMSO as compared with the groups treated with 5-HTP and KET (18.30 nmol; $p < 0.05$).

(C–F) No intergroup differences were observed in latency to AGSz, duration of tonic-clonic seizures, and seizure scores ($p > 0.05$). Compared with the vehicle group, the duration of wild running plus clonic seizures (W + C) was remarkably reduced in the group 5-HTP + 25% DMSO ($p < 0.05$).

(G) Representative images of cannula implantation in DBA/1 mice for ICV delivery.

S-IRA was significantly increased under the same parameters for DR photostimulation ($n = 7$, $p < 0.05$), indicating that the lower incidence of PTZ-induced S-IRA upon the photostimulation of the DR was significantly reversed by blocking 5-HT_{2A}R in the brain (Figure 5).

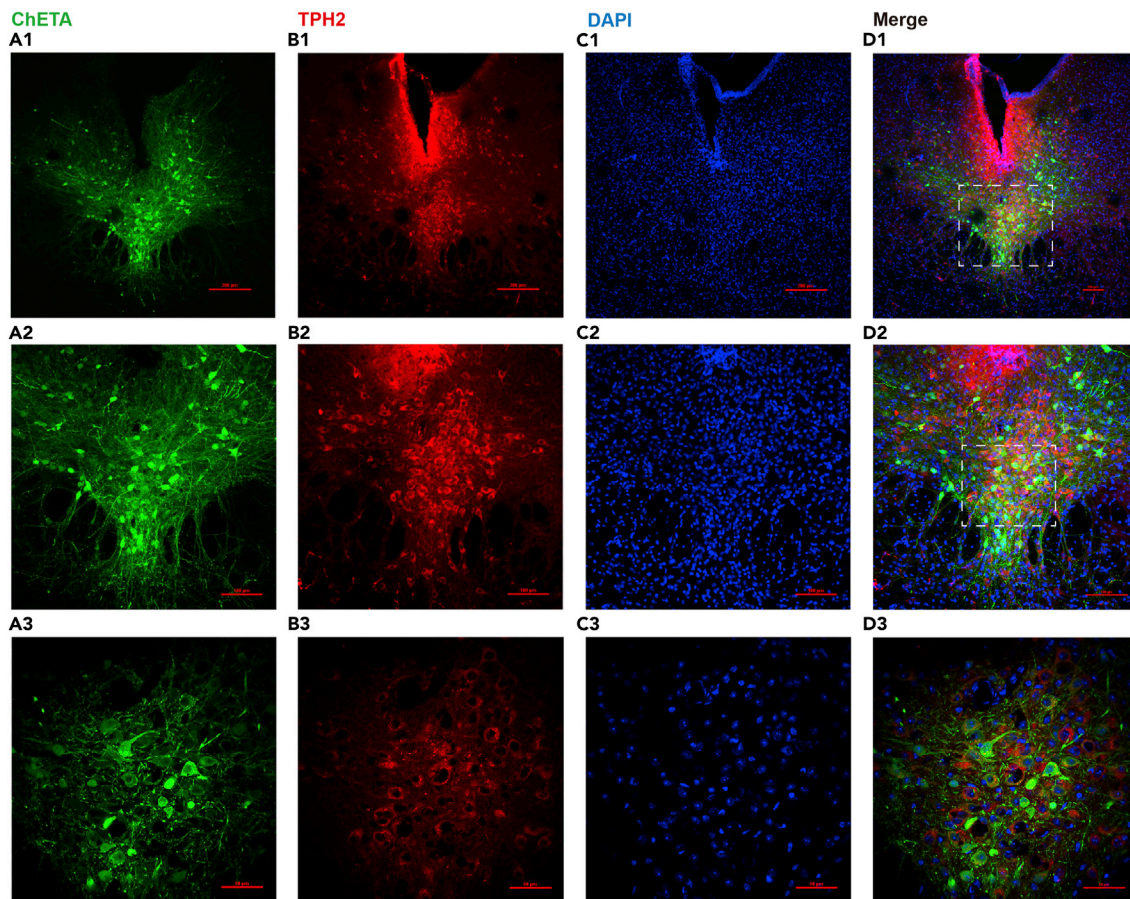


Figure 3. Localized expression of ChETA in 5-HT neurons in the DR of DBA/1 mice

(A1, A2, and A3) Neuronal immunostaining of EYFP, a surrogate marker for ChETA, in 5-HT neurons in the DR of a coronal brain slice. (B1, B2, and B3) Immunostaining of TPH2, a key enzyme for 5-HT synthesis in the CNS. (A1, B1, C1-3 and D1-3) merged images showing the co-expression of TPH2 and EYFP in 5-HT neurons. These data demonstrate that ChETA was restrictively expressed on the surface of 5-HT neurons in the DR ($n = 3$). Confocal image magnifications: a1-d1, 10 \times ; a2-d2, 20 \times ; a3-d3, 40 \times .

Activation of 5-HT neurons in the dorsal raphe nucleus produced differential effects on electroencephalogram activity in the seizure-induced respiratory arrest model with and without ketanserin treatment

Based on the above findings in the same experimental groups, we further examined the effect of activating 5-HT neurons in the DR on EEG activity in our mouse model of S-IRA with and without KET treatment. Compared with the group not exposed to photostimulation, the EEG activity was significantly reduced upon the photostimulation of 5-HT neurons in the DR of the mouse model. Analysis of the EEG wave data showed that the delta wave was significantly reduced by photostimulation ($p < 0.01$), and this effect was reversed by KET treatment ($p < 0.05$). No changes in the theta, alpha, beta, or gamma waves were apparent among the different treatment groups. These findings regarding EEG activity may reflect the specificity of 5-HT_{2A}R in the brain for modulating S-IRA and SUDEP (Figure 6).

Reduction in seizure-induced respiratory arrest upon the photostimulation of the dorsal raphe nucleus was dependent on 5-HT_{2A}R located in the pre-Bötzinger complex

Although the incidence of S-IRA was reduced by 5-HTP and by the photostimulation of the DR and this effect was significantly reversed by both IP and ICV injection of KET, it still needed to determine whether 5-HT_{2A}R in the PBC participated in mediating the process of S-IRA and SUDEP. Compared with the control group without the photostimulation of the DR and microinjection of 25% DMSO (400 nL) into the bilateral PBC, the incidence of PTZ-induced S-IRA was significantly reduced in the group with the photostimulation of the DR with the microinjection of 25% DMSO (400 nL) into the bilateral PBC ($p < 0.01$).

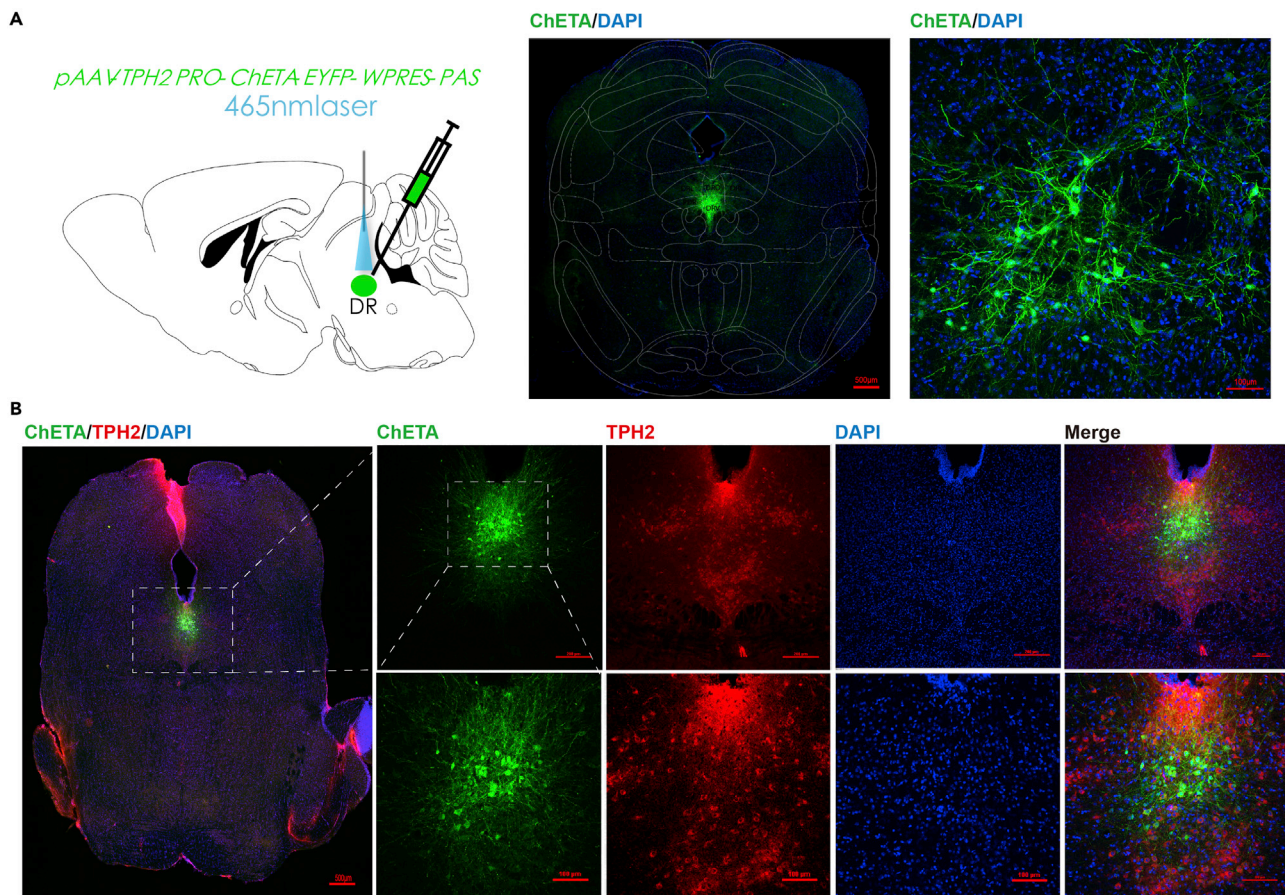


Figure 4. Placement of fiberoptic cannula tips in the DR

(A) An example of a coronal brain slice, showing the location of an optic fiber cannula tip and the expression of ChETA in the DR of a DBA/1 mouse, according to the mouse atlas of Paxinos and Franklin (fourth Edition, Paxinos, and Franklin, 2013).

(B) Neuronal immunostaining of co-expression of ChETA and TPH2 in the DR of a DBA/1 mouse. No thermal injury owing to PS was observed in the area around the optic fiber tips. No PS = no photostimulation; PS = photostimulation.

However, the incidence of PTZ-induced S-IRA upon the photostimulation of the DR with the microinjection of 25% DMSO (400 nL) into the bilateral PBC was 14.28%, whereas that with the photostimulation of the DR and microinjection of KET (400 nL) into the bilateral PBC was 85.71% ($p < 0.01$) (Figure 7B). No significant intergroup differences ($p > 0.05$) were observed in latency to AGSz ($p > 0.05$). Duration of wild-running and clonic seizures was significantly shorter in the control group without the photostimulation of the DR and microinjection of 25% DMSO (400 nL) into the bilateral PBC, compared with the other two groups ($p < 0.01$). Duration of tonic seizures and seizure scores were significantly less in the group treated with the photostimulation of the DR and microinjection of 25% DMSO (400 nL), compared with the control group ($p < 0.001$, $p < 0.01$) and the group treated with the photostimulation of the DR and microinjection of KET (400 nL) ($p < 0.001$, $p < 0.001$) (Figures 7C-7F). Subsequently, the existence of the neural circuit between the DR and the PBC was verified by using the nerve tracer CTB-555. For DR injection CTB-555, the quantification of CTB(+)/NK1R(+)/5-HT2AR(+) cells in PBC is 73.14%. For PBC injection CTB-555, the quantification of CTB(+)/NK1R(+)/5-HT2AR(+) cells in DR is 32.36%. Optogenetic activation of this neural circuit was shown to contribute to the inhibition of S-IRA and combined with previous pharmacological experiments, 5-HT2AR in the PBC might be a specific target for preventing SUDEP (Figures 8 and 9). We speculated that the serotonergic neurotransmission resulting from the optogenetic activation of the DR was accelerated between the DR and PBC, resulting in the release of more 5-HT within the PBC to activate 5-HT2AR, which restored the normal respiratory rhythm to protect against S-IRA and SUDEP.

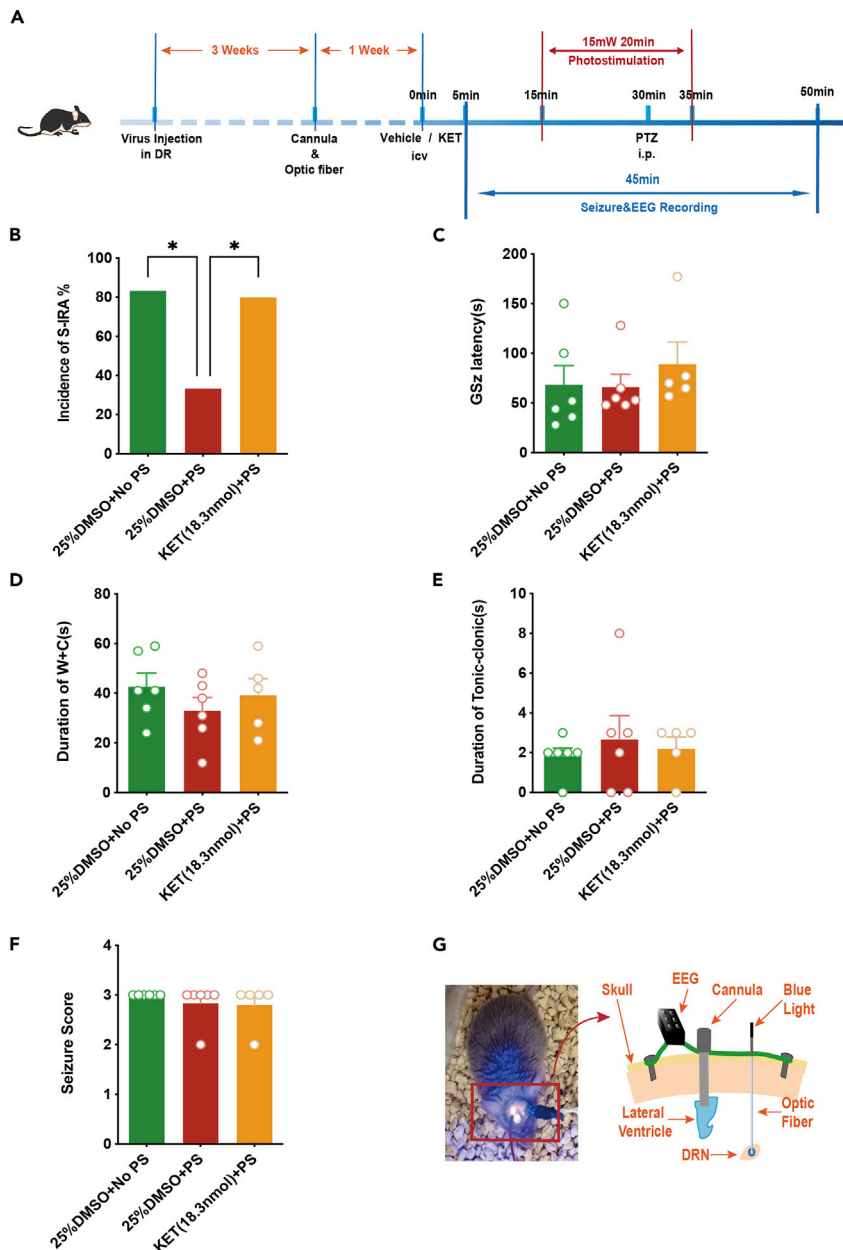


Figure 5. Optogenetic activation of TPH2-ChETA neurons in DR-mediated reduction of PTZ-induced S-IRA was significantly reversed by ICV injection of KET without changing seizure behavior

(A) Schematic illustration of the pAAV-TPH2-PRO-ChETA-EYFP-WPRES-PAS delivery into the DR of DBA/1 mice and implantation of the optic fiber and cannula to receive PS of the DR and record the changes in EEG upon ICV injection of KET.

(B) Compared with the control group treated with PTZ and no PS, the incidence of PTZ-induced S-IRA was significantly reduced by PS ($n = 7$ and $n = 6$, respectively; $p < 0.05$). However, the lower incidence of S-IRA after PS was remarkably reversed by ICV injection of KET at a dose of 18.3 nmol ($n = 6$ and $n = 7$, respectively; $p < 0.05$).

(C–F) No obvious differences between groups were observed in the analysis of seizure score, duration of wild running and clonic seizure, AGSz latency, and duration of tonic seizures.

(G) Representative images of implanted EEG, ICV, and optic fiber devices in a DBA/1 mouse. No PS, no photostimulation; PS, photostimulation.

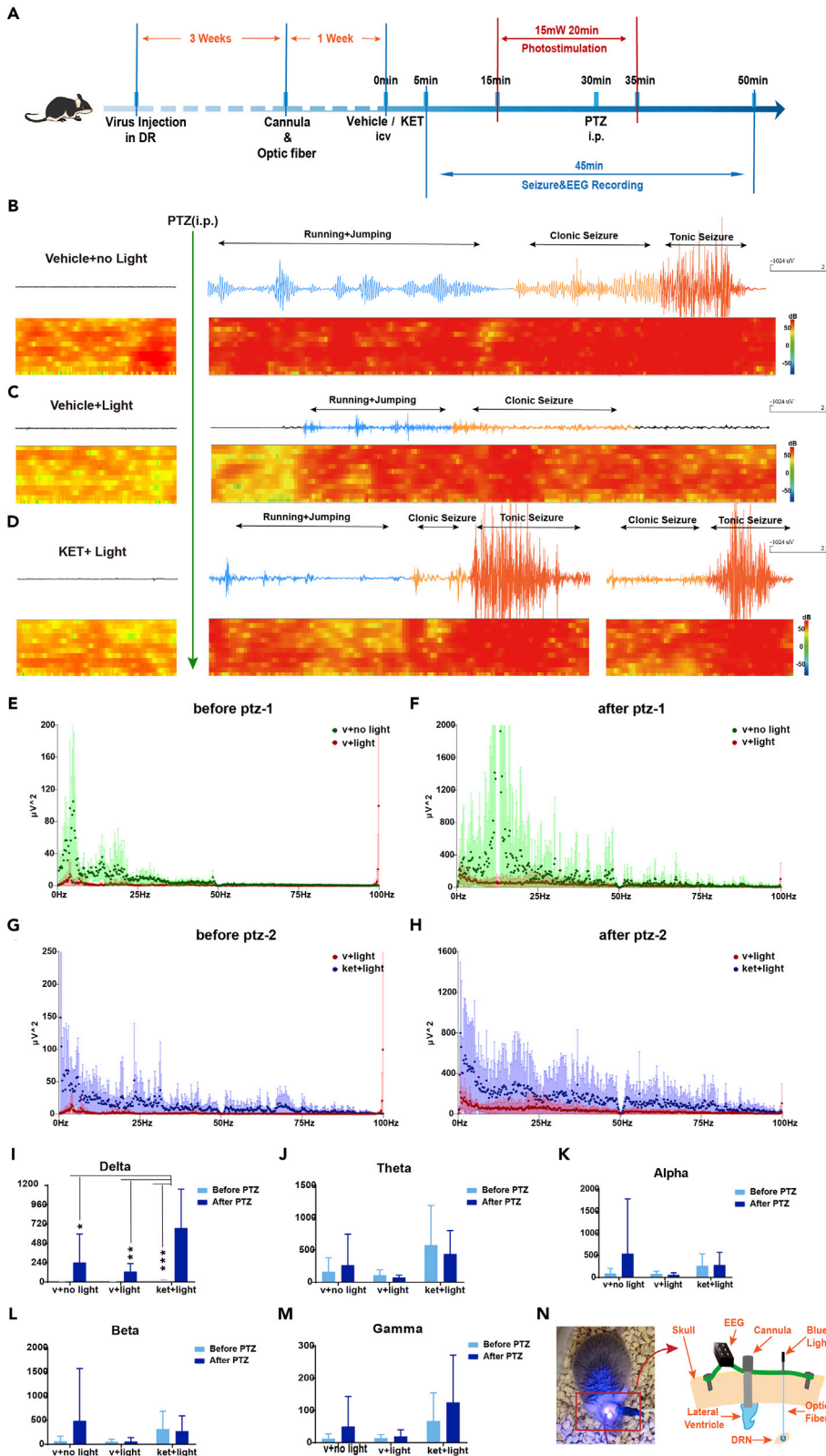


Figure 6. EEG activity upon the optogenetic activation of TPH2-ChET

(A) neurons in the DR-mediated reduction of PTZ-induced S-IRA and significant reversal of this reduction after ICV injection of KET. A schematic illustration of the pAAV-TPH2-PRO-ChETA-EYFP-WPRES-PAS delivery into the DR of DBA/1 mice and implantation of the optic fiber and cannula to receive PS of the DR and record changes in EEG upon ICV injection of KET.

(B–D) Compared with the control group that received PTZ without PS, the EEG activity during the clonic and tonic seizure stages was significantly suppressed in the group treated with PTZ and PS. Furthermore, this suppression of EEG activity was significantly increased in the group treated with PTZ, PS, and ICV microinjection of KET.

(E–M) Delta wave of EEG activity was significantly reduced by light and reversed by KET.

(N) Representative images of implanted EEG, ICV, and optic fiber devices in a DBA/1 mouse. Light, photostimulation; No light, no photostimulation; PS, photostimulation.

Photostimulation increased c-fos expression in 5-HT neurons in the dorsal raphe nucleus

To investigate whether photostimulation increased the excitability of 5-HT neurons in the DR, we examined the neuronal expression of c-fos, an immediate-early gene that was widely accepted as a marker for neuronal activity in optogenetics studies, in the DR of DBA/1 mice with and without photostimulation. Compared with the level of c-fos expression in 5-HT neurons in the DR of DBA/1 mice without photostimulation ($n = 2$), c-fos expression in these neurons was significantly increased with photostimulation (20-ms pulse duration, 20 Hz, at 15 mW for 20 min, $n = 2$, $p < 0.05$). This result indicated that the reduction in S-IRA induced by photostimulation occurred via activation of 5-HT neurons (Figure 10).

Photostimulation of the bilateral pre-Böttinger complex did not significantly reduce the incidence of pentylenetetrazole-induced seizure-induced respiratory arrest

We next investigated whether the incidence of PTZ-induced S-IRA after the photostimulation of the bilateral PBC could be independently reduced by the photostimulation of TPH2-ChETA neurons in the bilateral PBC. Although the incidence of PTZ-induced S-IRA was reduced by the photostimulation of the bilateral PBC, no significant difference was observed between the control group treated with PTZ and no photostimulation and the group treated with PTZ together with photostimulation ($n = 6$ and $n = 7$, respectively, $p > 0.05$). Additionally, no significant difference was observed between the control group treated with PTZ, no photostimulation, and microinjection of vehicle, and the group treated with PTZ, photostimulation, and microinjection of 4 μ g KET ($n = 7$ and $n = 3$, respectively, $p > 0.05$) (Figure 11G). Also, no significant intergroup differences ($p > 0.05$) were observed in latency to AGSz, duration of wild running and clonic seizures, duration of tonic-clonic seizures, and seizure scores (Figures 11H–11K). These findings suggested that while the activation of the neural circuit between the DR and PBC could significantly reduce the incidence of S-IRA, photostimulation of only the PBC did not significantly reduce the incidence of S-IRA and SUDEP in our model (Figure 11), suggesting that the limited increase in 5-HT content caused by exclusive photostimulation of the PBC to boost the 5-HT level in the PBC did not maintain the normal respiratory rhythm to protect against S-IRA and SUDEP.

Pentylenetetrazole-induced neuronal activity in pre-Böttinger complex during seizures was significantly reduced by the photostimulation of the dorsal raphe nucleus based on photometry recordings

Calcium signaling within neurons of the bilateral PBC was recorded by photometry in mice infected with GCaMP6f in the bilateral PBC without photostimulation in DR during the clonic and tonic seizure phases evoked by PTZ. There was no significant difference in peak $\Delta F/F$ of PBC between the clonic seizures of the photostimulation group and vehicle group ($p > 0.05$, Figures 12E–12G). Compared with the vehicle group, peak $\Delta F/F$ of tonic seizures was significantly decreased in the photostimulation group ($p < 0.05$, Figures 12H–12J). These data indicated that the photostimulation of the DR could reduce abnormal calcium signaling activity in the bilateral PBC, which could serve to normalize respiration rhythm and thereby prevent S-IRA and SUDEP (Figure 12).

Ketanserin microinjection into the bilateral pre-Böttinger complex at the treatment dose does not cause death in DBA/1 mice

We explored whether therapeutic doses of KET were lethal. And we found that KET microinjection into the bilateral PBC at the treatment dose (400 nL) in DBA/1 mice did not cause death. This data showed that the above doses of KET did not affect our model (Figure S1).

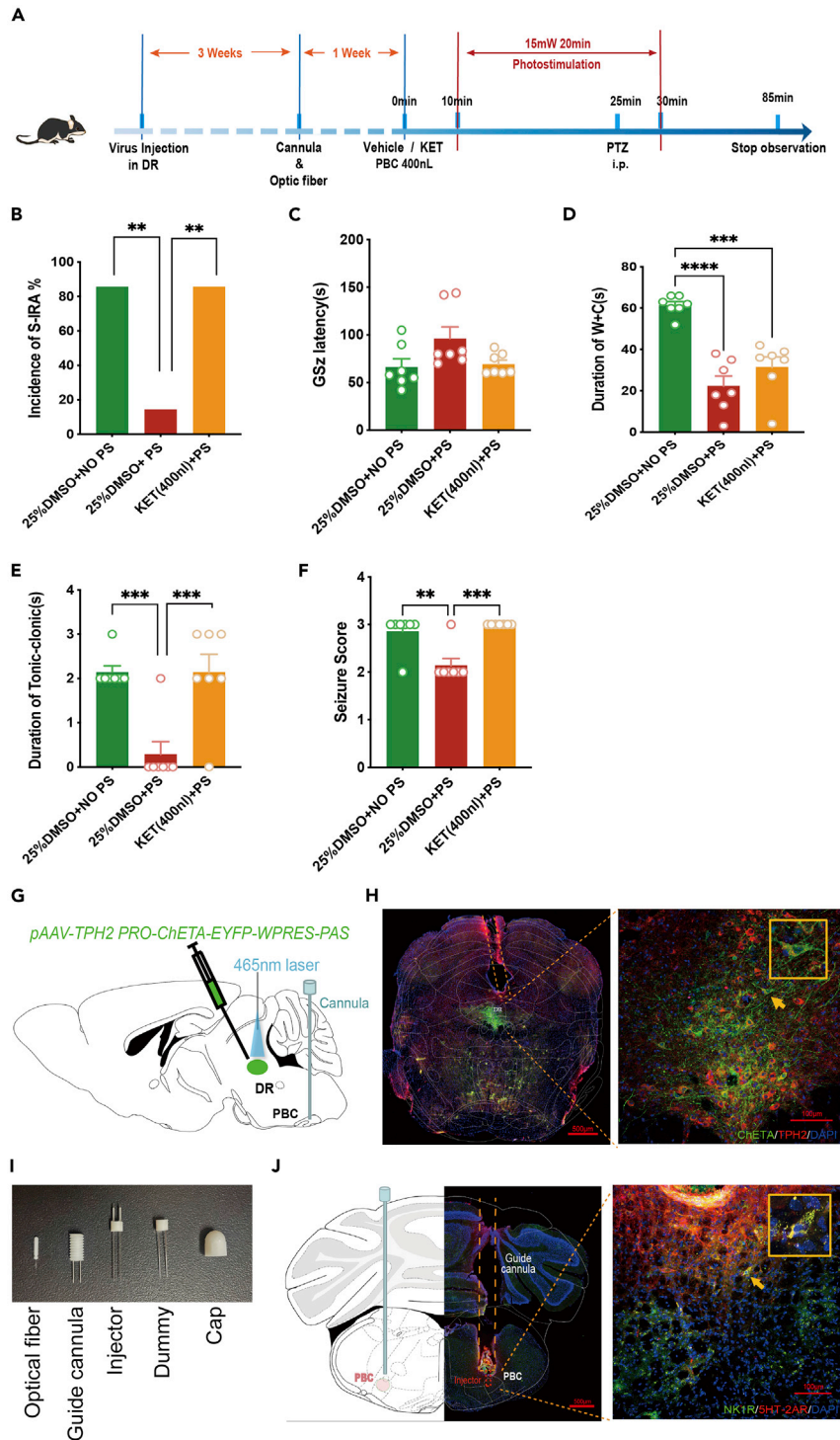


Figure 7. Optogenetic activation of TPH2-ChETA neurons in DR-mediated reduction of PTZ-induced S-IRA was significantly reversed by the injection of KET into the PBC

(A) Schematic illustration of the pAAV-TPH2 PRO-ChETA-EYFP-WPRES-PAS delivery into the DR of DBA/1 mice and implantation of the optic fiber into the DR and cannula into the bilateral PBC to receive PS of the DR.
(B) Compared with that in the control group treated with PTZ without PS with a microinjection of 400 nL 25% DMSO into the bilateral PBC, the incidence of PTZ-induced S-IRA was significantly reduced in the group injected PTZ with PS in the DR with microinjection of 400 nL 25% DMSO into the bilateral PBC (n = 7 and n = 6, respectively; p < 0.01). Compared with

Figure 7. Continued

the group with PTZ with PS in the DR with microinjection of 400 nL 25% DMSO into the bilateral PBC, the incidence of PTZ-induced S-IRA was significantly reduced in the group with PTZ that received PS and microinjection of 400 nL KET into the bilateral PBC ($n = 6$ and $n = 7$, respectively; $p < 0.01$).

(C) No obvious differences were observed between treatment groups in the GSz latency (s) ($p > 0.05$).

(D) Duration of wild running and clonic seizure in the group with 25% DMSO + NO PS was significantly higher than the group with 25% DMSO + PS and the group with KET 400 nL + PS ($p < 0.001$ and $p < 0.001$, respectively).

(E and F) The seizure score or duration of tonic seizures in the group with 25% DMSO + PS was significantly reduced compared to the group with 25% DMSO + NO PS and the group with KET 400 nL + PS ($p < 0.01$ and $p < 0.001$, respectively).

(G–J) Representative images of the delivery of pAAV-TPH2 PRO-ChETA-EYFP-WPRES-PAS into the DR and injection of KET into the bilateral PBC.

(H) Staining of ChETA, TPH2, and DAPI in the DR.

(I) All implantation devices in a DBA/1 mouse.

(J) The tracks for KET injection into the bilateral PBC and staining for NK1R, 5-HT2AR, and DAPI in the bilateral PBC. No PS, no photostimulation; PS, photostimulation.

5-hydroxytryptophan mediated reduction in pentylenetetrazole-induced seizure-induced respiratory arrest was significantly reversed by the bilateral pre-Bötzing complex microinjection of ketanserin

Compared with the group pretreated with 5-HTP and 25% DMSO, the incidence of S-IRA was significantly increased in the vehicle control group ($p < 0.01$) and 5-HTP + KET group ($p < 0.05$), which indicated that 5-HTP mediated reduction in PTZ-induced S-IRA was significantly reversed by the bilateral PBC microinjection of KET. Moreover, the GSz latency was significantly increased in the group treated with 5-HTP + KET (400 nL) as compared with the group treated with 5-HTP and 25% DMSO ($p < 0.05$). Compared with the vehicle group, the duration of wild running plus clonic seizures (W + C) was significantly increased in the group treated with 5-HTP and 25% DMSO ($p < 0.001$) and the group treated with 5-HTP and KET ($p < 0.01$). There were no significant intergroup differences in the duration of tonic-clonic seizures and seizure scores (Figure S2). These data indicate that a lower incidence of S-IRA by PTZ via an increase in the content of 5-HTP was reversed by the blocked 5-HT_{2A} receptor in the brain (Figure S2).

Photostimulation of TPH2-ChETA neurons in dorsal raphe nucleus of DBA/1 mice mediated reduction in pentylenetetrazole-induced seizure-induced respiratory arrest and c-fos expression was significantly increased in pre-Bötzing complex

In order to further verify the connection between DR and PBC, we gave photostimulation at DR and observed the changes in c-fos at PBC. Our data showed that the incidence of S-IRA, duration of tonic-clonic seizures, and seizure scores were remarkably reduced in the photostimulation group compared to the control group ($p < 0.05$, $p < 0.01$, $p < 0.01$). The GSz latency was significantly increased in the photostimulation group than in the control group ($p < 0.05$). These data indicated that the photostimulation of TPH2-ChETA neurons in DR of DBA/1 mice mediated reduction in PTZ-induced S-IRA. Furthermore, the count of c-fos(+)/5-HT_{2AR}(+) cells was observed more in the PS group than in the No PS group ($p < 0.001$). This data strongly verified the hypothesis of SUDEP might be mediated by a reciprocal connection between 5-HT neurons of the DR and PBC (Figure S3).

DISCUSSION

SUDEP is a fatal complication of epilepsy, and although initial advances in understanding the role of 5-HT in the nervous system have helped to identify some causes of SUDEP, the pathogenesis of SUDEP remains poorly understood (Devinsky et al., 2016; Lhatoo et al., 2015; Massey et al., 2014; Ryvlin et al., 2013). Our previous study showed that the administration of 5-HTP significantly reduced the incidence of S-IRA via anti-convulsant effects (Vilella et al., 2019; Zhao et al., 2019). This indicated that most treated DBA/1 mice avoided S-IRA without experiencing tonic-clonic seizures other than wild running and generalized clonic seizures, and thus remained sensitive to some seizures.

Different from our previous study in which atomoxetine reduced the incidence of S-IRA evoked by acoustic stimulation without affecting seizure behavior in DBA/1 mice (Zhang et al., 2017, 2018), administration of 5-HTP significantly reduced the incidence of S-IRA through its anti-convulsant effects in our models. Such an anti-convulsant effect of 5-HTP is basically consistent with other studies showing that the activation of 5-HT neurons can reduce the severity of seizures (Ozawa and Okado, 2002; Peña and Ramirez, 2002).

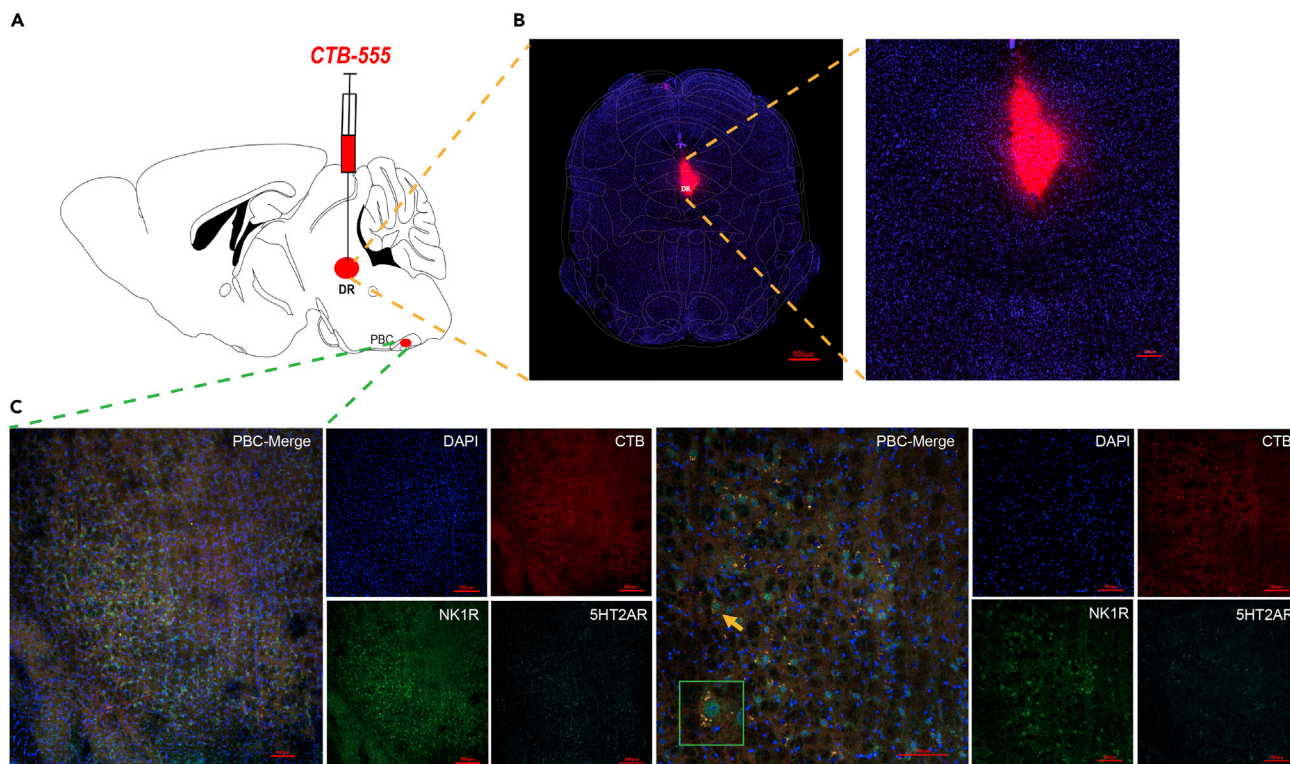


Figure 8. Neural projection from the DR to the PBC was established by the application of the nerve tracer CTB-555

(A and B) Representative coronal brain slice, showing the location of CTB-555 injection in the DR.

(C) Projection of the DR to the PBC with co-expression of CTB, NK1R, and 5-HT2AR (n = 3).

Other groups showed that boosting the 5-HT level in the brain suppresses seizures via anti-convulsant effects as well (Donato Di Paola et al., 2007; Osipova et al., 2010). However, the administration of KET increased the incidence of S-IRA in response to acoustic stimulation or PTZ injection even after 5-HTP treatment with the occurrence of partly wild running, clonic, and/or tonic-clonic seizures, which demonstrated that IP administration of KET reversed the reduction of the incidence of S-IRA by 5-HTP and only partly affected seizure behaviors by acting on the neuron nucleus controlling respiratory activity. First, we proved through pharmacological experiments that the peripheral injection of 5-HTP can significantly reduce the incidence of S-IRA, and this effect can be reversed by IP injection of a certain concentration of KET. Although KET reversed the suppressive effect of 5-HTP on S-IRA in a dose-dependent manner in the PTZ injection model, a ceiling effect was observed for the ability of KET to reverse the 5-HTP-mediated reduced incidence of S-IRA in the acoustic stimulation SUDEP model.

In order to further study the reversal effect of KET, we injected KET into the lateral ventricle and also observed that the dosage of the reversal effect of KET produced no effects on the mortality rate of DBA/1 mice. However, the inhibitory effect of 5-HTP against S-IRA was significantly reversed by the same dosage of KET. The results showed that KET reversed the suppressive effects of 5-HTP both via IP injection and ICV injection, suggesting that the reversal effect of KET is independent of the SUDEP model type. Combined with the previous research, two case reports of SUDEP have demonstrated ictal oxygen desaturation in about a third of patients with intractable epilepsy and hypoventilation (Bateman et al., 2008, 2010b), indicating that the recovery of ventilation function plays an important role in reversing S-IRA. In addition, animal studies suggest that *Lmx1bf/f/p* mice, with genetically deleted brainstem serotonergic neurons, often suffer postictal respiratory arrest that can be prevented by 5-HT2AR agonists (Damasceno et al., 2013).

Considering that PBC plays a key role in modulating respiratory rhythm, the nucleus of PBC in the brainstem mainly involved in the regulation of respiratory and neurotransmission of serotonin in the above cases should be a stronger candidate. Furthermore, a previous study showed that the activation of 5-HT2 B

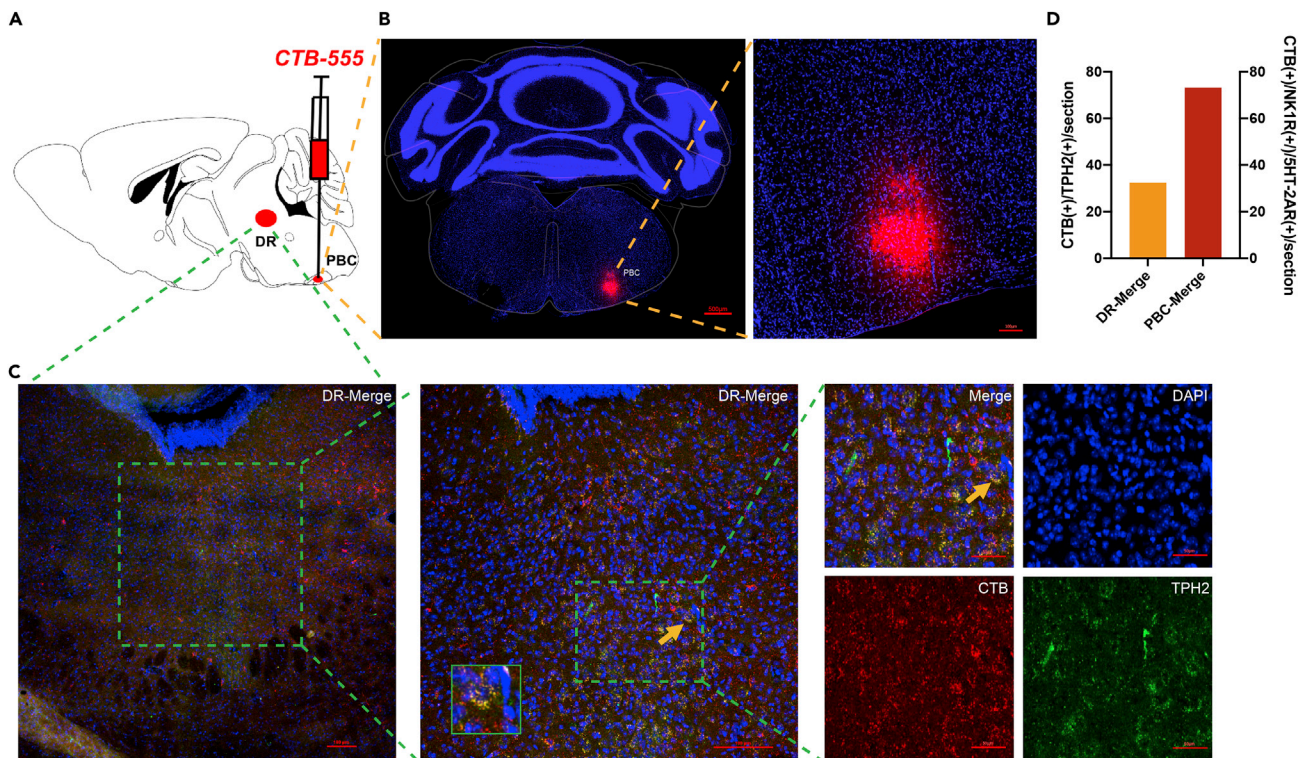


Figure 9. Neural projection from the PBC to the DR was established by the application of the nerve tracer CTB-555

(A and B) Representative coronal brain slice, showing the location of CTB-555 injection in the PBC.

(C) Projection of the PBC to the DR with co-expression of TPH2 and CTB-555.

(D) Quantification of CTB(+)/NK1R(+)/5-HT2AR(+) cells in DBA/1 mice with DR injection CTB-555 and PBC injection CTB-555. For DR injection CTB-555, the quantification of cells in PBC is 73.14% (n = 3). For PBC injection CTB-555, the quantification of cells in DR is 32.36%.

and C by different doses of mCPP, a 5-HT_{2B/2C} receptor agonist, even the toxic dose, produced no effects on the S-IRA in the DBA/1 mice models which is the same to our DBA/1 mice SUDEP models (Faingold et al., 2011). Based on this, we propose that KET mainly acts on the 5-HT_{2AR} in the PBC and inhibits the neurotransmission of serotonin in the brain. To test this hypothesis, we further microinjected KET into the PBC to observe its effect on the incidence of S-IRA.

Meanwhile, most DBA/1 mice in the different treatment groups recovered from S-IRA within 24–72 h, indicating that the recovery interval for S-IRA depends on the concentration of 5-HT in the brain. In addition, we observed a dose-dependent effect on the reversal of the effect of 5-HTP on the S-IRA incidence and a ceiling effect with 25 mg/kg KET (IP). Indeed, our previous study showed that the reduced incidence of S-IRA achieved via activating 5-HT neurons in the DR by optogenetics was significantly reversed by ondansetron, a specific antagonist of the 5-HT₃ receptor (Zhao et al., 2019). However, we cannot rule out the possibility that 5-HT_{2AR} mediates the pathogenesis of S-IRA and SUDEP by closely interacting with 5-HT₃ receptor (5-HT_{3R}) in the brain. Further research is needed to characterize the interaction between 5-HT_{2AR} and the 5-HT_{3R}. Other 5-HT receptors expressed in the respiratory network have also been implicated in the control of breathing. For example, 5-HT_{1A} receptors are extensively expressed (Richter et al., 2003), and 5-HT_{1A} agonists inhibit some respiratory neurons (Lalley et al., 1994), including some PBC neuron cells (Schwarzacher et al., 2002).

Previously an SSRI also was shown to be effective at reducing S-IRA evoked by maximal electroshock (MES) in *Lmx1b(f/f)* mice on a primarily C57BL/6J background, a strain that is resistant to AGSz, and depletion of 5-HT neurons enhanced seizure severity, which led to S-IRA and could be prevented by 5-HT_{2AR} activation through IP injection of with DOI (2,5-dimethoxy-4-iodophenylpropane hydrochloride), a selective agonist for 5-HT_{2AR}, in an MES model (Bateman et al., 2010a). However, it remained unclear whether depleting 5-HT neurons itself led to S-IRA or the reversal effects by DOI targeting peripheral or central 5-HT_{2AR}.

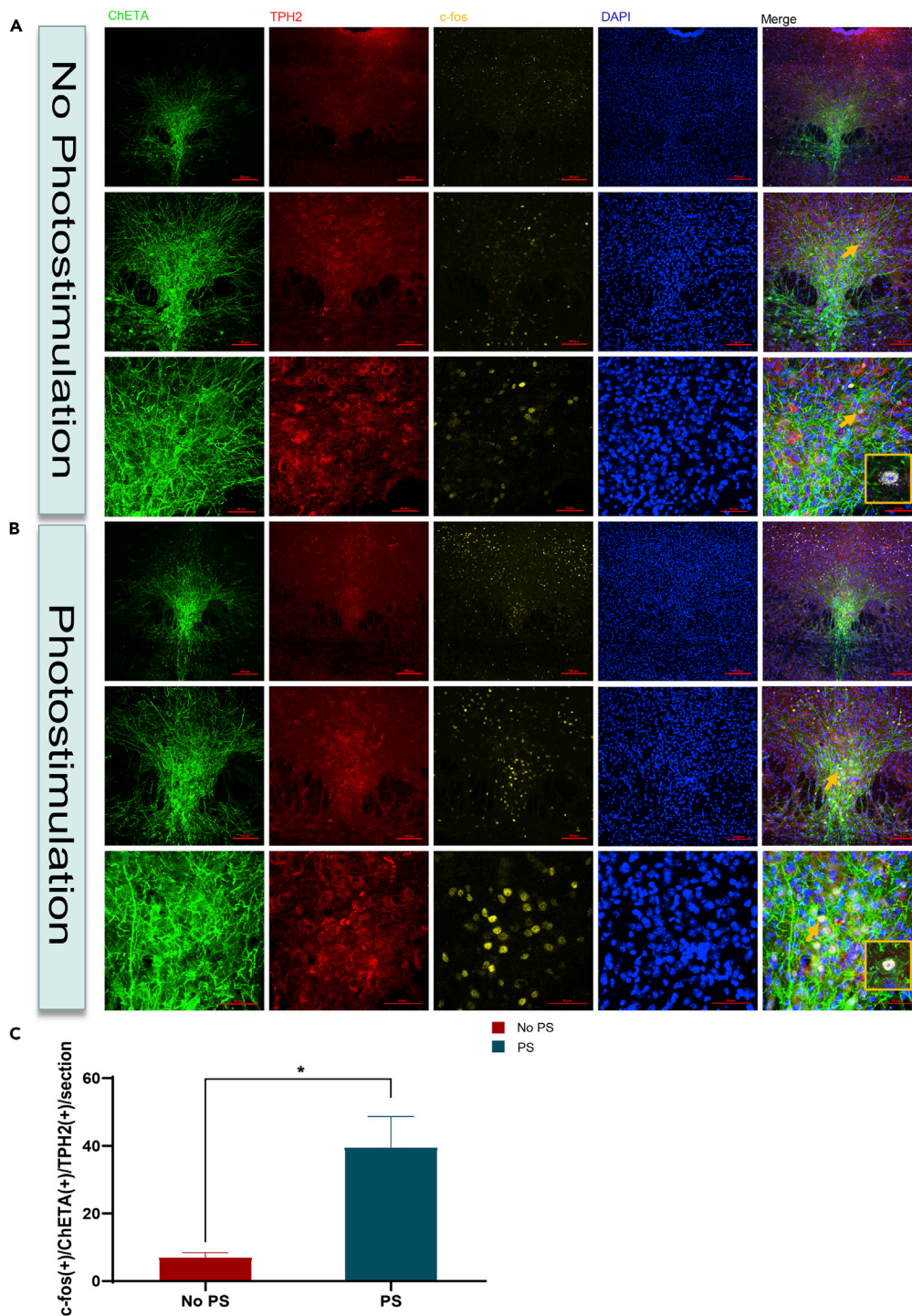


Figure 10. c-fos expression was significantly increased in the DR by the photostimulation of TPH2-ChETA neurons in the DR of DBA/1 mice

(A) Neuronal immunostaining showing co-localization of c-fos, TPH2, and EYFP in a DBA/1 mouse that underwent the implantation of a fiber optic cannula without PS (n = 2).
 (B) Immunostaining showing the co-localization of c-fos, TPH2, and EYFP in a DBA/1 mouse exposed to PS at 15 mW for 20 min (n = 2).
 (C) Quantification of c-fos(+)/EYFP(+)/TPH2(+) cells in DBA/1 mice with and without PS. Significantly more c-fos(+)/EYFP(+)/TPH2(+) cells were observed in the PS group than in the No PS group ($p < 0.05$). No PS, no photostimulation; PS, photostimulation.

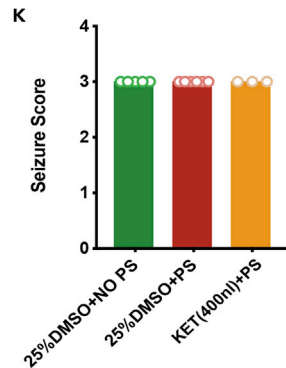
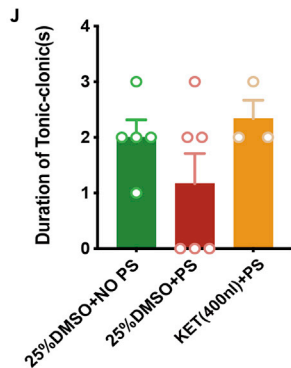
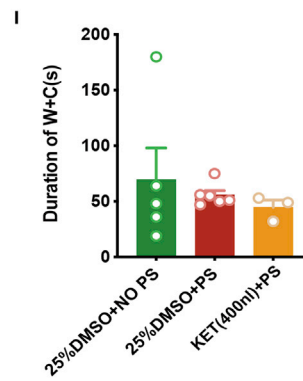
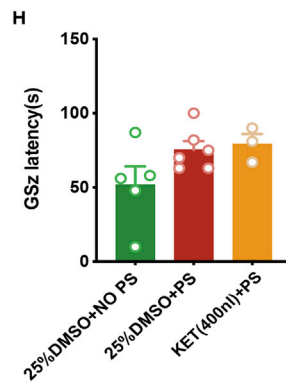
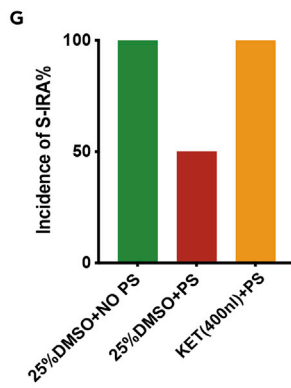
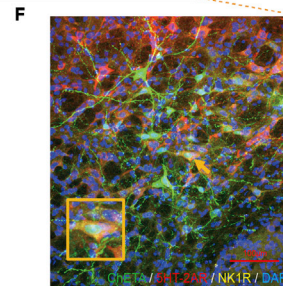
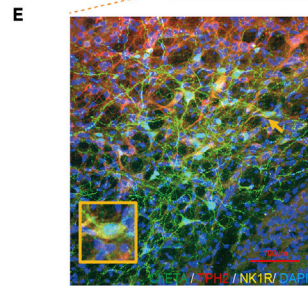
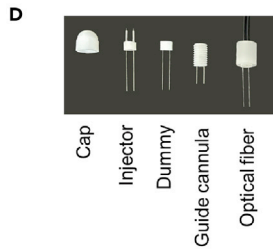
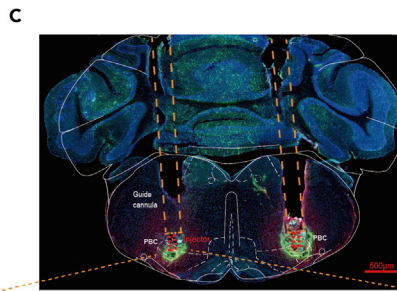
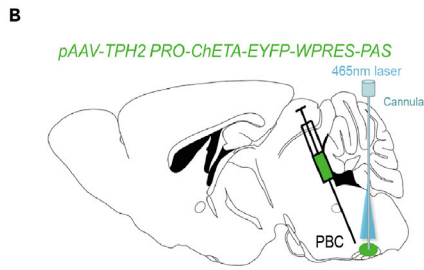
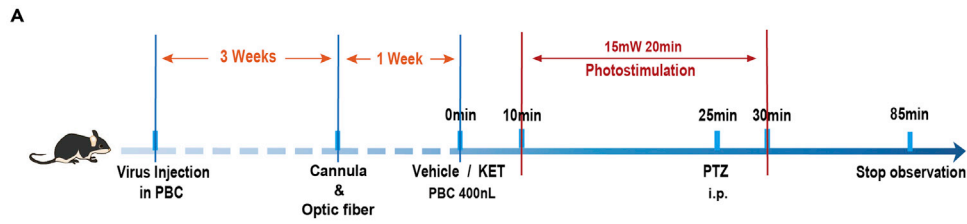


Figure 11. Activation of ChETA-TPH2 neurons in the PBC could have an effect on S-IRA but did not significantly reduce the incidence of S-IRA in DBA/1 mice or prevent death

(A) Schematic illustration of the pAAV-TPH2-PRO-ChETA-EYFP-WPRES-PAS delivery into the bilateral PBC of DBA/1 mice and implantation of the optic fiber and cannula to receive PS of the PBC and observe changes in the incidence of PTZ-induced S-IRA upon the microinjection of KET in the PBC.

(B–F) The tracks of optic fibers with cannula implanted into each side of the bilateral PBC and staining for ChETA, TPH2, NK1R, 5-HT2AR, and DAPI expression in the bilateral PBC.

(G) Compared with that in the control group treated with PTZ without PS, the incidence of PTZ-induced S-IRA was not significantly reduced by PS of the bilateral PBC ($p > 0.05$). Furthermore, no significant differences were observed between the group with PS and microinjection of vehicle into the bilateral PBC and the group with PS and microinjection of KET into the bilateral PBC ($p > 0.05$).

(H–K) No obvious differences between treatment groups were observed in the seizure score, duration of wild running and clonic seizure, AGSz latency, duration of tonic seizure, or seizure score ($p > 0.05$). No PS, no photostimulation; PS, photostimulation.

By contrast, based on our previous findings, we further explored the role of 5-HT neurotransmission and 5-HT2AR by peripheral and central intervention approaches with KET in different SUDEP models. Thus, according to our findings, the role of 5-HT2AR in modulating S-IRA is supported by the results from the MES model, which further strengthens our understanding of the role of 5-HT in the pathogenesis of S-IRA and SUDEP, which will aid the future design of therapeutic strategies to prevent SUDEP.

Previous studies have suggested that 5-HT neurons in DR project widely to other brain regions. However, 5-HT2A receptors located in different brain regions play different roles by binding with 5-HT. The 5-HT2A receptors are highly expressed in the prefrontal cortex (PFC), where a striking overlapping laminar distribution of 5-HT2A and mGlu2/3 receptors has been reported by a number of studies and led to the hypothesis that 5-HT2A and mGlu2/3 receptors share close functional interactions with physiological relevance by modulating cortical activity and local network oscillations (Aghajanian and Marek, 1999; Gewirtz and Marek, 2000; Marek et al., 2000).

Numerous psychiatric and neurodegenerative diseases result in disrupted executive function (Aznar and Hervig, 2016). In addition, data on the presence of 5-HT2AR mRNA in PFC neurons that project to the ventral tegmental area in the rat are relevant for the understanding of the mechanism of action of atypical antipsychotic drugs (Mengod et al., 2015). Animal and human studies have linked these disorders with alterations in the 5-HT2AR system, making this an important pharmacological target for the treatment of disorders with impaired cognitive function. Besides, the administration of selective serotonin reuptake inhibitors (SSRIs) and other compounds that increase serotonin, both systemically and locally in the auditory cortex, to decrease the magnitude of the loudness-dependent auditory evoked potential (LDAEP), electroencephalography (EEG) measure originating from the primary auditory cortex (Hegerl and Juckel, 1993; Juckel et al., 2007; Kähkönen et al., 2002; Nathan et al., 2006; Wutzler et al., 2008). Taken together, these findings suggest that 5-HT modulates auditory cortex function.

Animal studies have shown that 5-HT decreases GABAergic neurotransmission pre- and post-synaptically in the primary auditory cortex via 5-HT1A and 5-HT2A receptors, respectively, and decreases the firing rate of pyramidal cells in juvenile rats (García-Oscos et al., 2015; Rao et al., 2010). Previous studies have shown that a voltage-dependent persistent sodium current (INaP) is augmented in PBC neurons of neonatal mice by the activation of 5-HT2A receptors and administration of KET has been found to attenuate baseline inspiratory rhythmic activity *in vitro* in slices from neonatal mice, implicating the involvement of 5-HT2A receptors (Peña and Ramirez, 2002).

Based on these studies, 5-HT2A receptors in different brain regions play various physiological roles, but those located in PBC mainly regulate respiration. To further exclude other 5-HT receptors in PBC that may involve in the regulation of S-IRA, a previous study cited by us will help to elucidate, which showed a 5-HT2B/2CR agonist mCPP was effective in blocking S-IRA without blocking seizures in DBA/2 mice, but mCPP was totally ineffective and even toxic in DBA/1 mice (Faingold et al., 2011). Taken together, 5-HT2A receptors in PBC are involved in the regulation of S-IRA in our models. Furthermore, the co-expression of c-fos and 5-HT2AR in PBC was significantly increased by the blue light activation of TPH2-ChETA neuron in DR. Of course, we cannot totally exclude KET by acting other receptors to play its role in our models. Thus, in the future, we will use more specific methods, such as gene knockout, to specifically intervene in the 5-HT2A receptors located in certain regions to explore its effect on S-IRA.

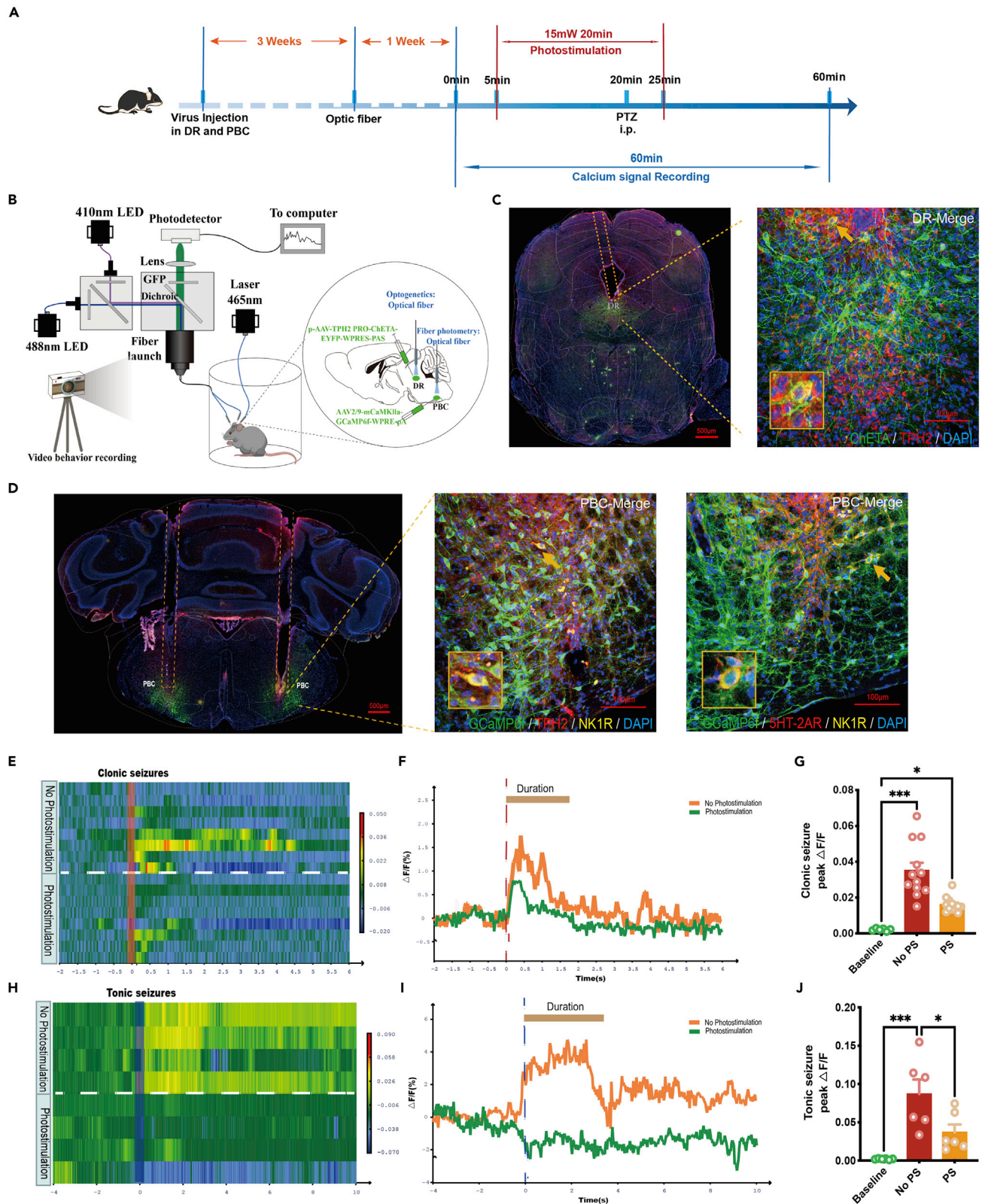


Figure 12. Photostimulation of the DR influenced calcium signaling in the PBC during PTZ-induced seizures

(A–D) Photometric recordings from all DBA/1 mice infected with ChETA and GCaMP6f in the DR and the bilateral PBC and of neural activity based on calcium signaling in the bilateral PBC. Shown are representative images of the tracks of optic fibers implanted into the DR and the bilateral PBC and staining for ChETA, TPH2 and GCaMP6f, NK1R, 5-HT2AR, and DAPI in the DR and bilateral PBC.

(E–J) In the group without PS of the DR, the activity wave of calcium signals from the bilateral PBC was strong during clonic and tonic seizures evoked by PTZ.

(E–G) There was no significant difference in peak $\Delta F/F$ of PBC between the clonic seizures of the photostimulation group and vehicle group ($p > 0.05$).

(H–J) Peak $\Delta F/F$ in PBC of tonic seizures was significantly decreased in the photostimulation group than in the control group ($p < 0.05$). PS, photostimulation.

Moreover, based on the localized expression of 5-HT2AR in the PBC, which plays an important role in modulating respiration rhythm, and on our previous finding that the incidence of S-IRA can be significantly reduced by the activation of TPH2-ChR2 neurons in the DR (Zhang et al., 2018), we further investigated the mechanisms of how the interaction between 5-HT and 5-HT2AR mediates S-IRA and SUDEP in the same models. For this study, we used optogenetics methods to test whether the activation of TPH2-ChETA neurons in the DR significantly reduced the incidence of S-IRA evoked by PTZ via activating 5-HT2AR in the PBC. In the present study, the reduction in the incidence of PTZ-induced S-IRA via optogenetic activation of TPH2-ChETA neurons in the DR was remarkably reversed by ICV injection of KET. Subsequently, the reduction in the incidence of PTZ-induced S-IRA by the photostimulation of the DR was significantly reversed by the microinjection of KET into the bilateral PBC, in turn, suggesting that the photostimulation of the DR remarkably reduced the incidence of S-IRA by activating 5-HT2AR in the PBC in our models.

To further examine the bridge between the DR and PBC and its role in modulating S-IRA in our models, CTB-555, a nerve tracer, was used to confirm and establish the neural circuit between the DR and PBC. The results confirmed that the reduction in the incidence of PTZ-induced S-IRA upon the photostimulation of the DR stems from the neural circuit between the DR and PBC. However, we only tested this using the photostimulation of the DR and direct inhibition of 5-HT2AR in the bilateral PBC in this study. Whether the activation of TPH2-neurons in the PBC can reduce the incidence of S-IRA still needs to be verified in subsequent experiments. Of course, the roles of other neural circuits between the DR and other brain structures involved in modulating S-IRA and SUDEP cannot be excluded from our models.

Other structures may be involved in modulating S-IRA and SUDEP in our models. The ventral respiratory column (VRC) generates rhythmical respiration and is divided into four compartments: the rostral ventral respiratory group (rVRG), caudal ventral respiratory group (cVRG), Bötzing complex (BC), and PBC (Smith et al., 2009). The results of the present study indicated that the serotonergic neurons in both the rostral and caudal raphe nuclei, including DR, projected throughout VRC. The serotonergic neurons in the DR directly projected to the VRC and activated the VRC neurons in order to induce an increase in respiratory frequency (Morinaga et al., 2019). Therefore, it is possible that DR may regulate respiratory and even epilepsy through other regions of VRC, except PBC. Nevertheless, our pharmacologic and optogenetic findings suggest that the neural circuit between the DR and PBC plays a key role in modulating S-IRA and SUDEP.

In addition, unlike in our pharmacology experiments, although S-IRA of DBA/1 mice was blocked in optogenetics experiments, most DBA/1 mice continued to have clonic and tonic seizures. Upon analyzing the cause for this difference, the specificity of optogenetics and the specific delivery of KET by both ICV injection and injection into the PBC may be a cause. Meanwhile, the incidence of S-IRA evoked by PTZ was significantly reduced by activating the neural circuit between the DR and PBC without changing EEG activities, which further reflects the specificity of S-IRA inhibition in optogenetic experiments.

Our data also showed that the activation of TPH2-ChETA neurons in the PBC is insufficient for significantly reducing the incidence of PTZ-induced S-IRA. Furthermore, the neuronal calcium signaling in the PBC during seizures induced by PTZ was significantly reduced by the photostimulation of the DR according to photometry recordings. Thus, the activation of the neural circuit between the DR and PBC can specifically prevent S-IRA and SUDEP.

The results of the present study suggest that the lowered incidence of PTZ-induced S-IRA achieved by the administration of 5-HTP can be significantly reversed by treatment with KET. Furthermore, the suppressive effects of the optogenetic activation of the serotonergic neural circuit between the DR and PBC on S-IRA also were obviously reversed by KET in the DBA/1 mouse model, suggesting that the serotonergic neural

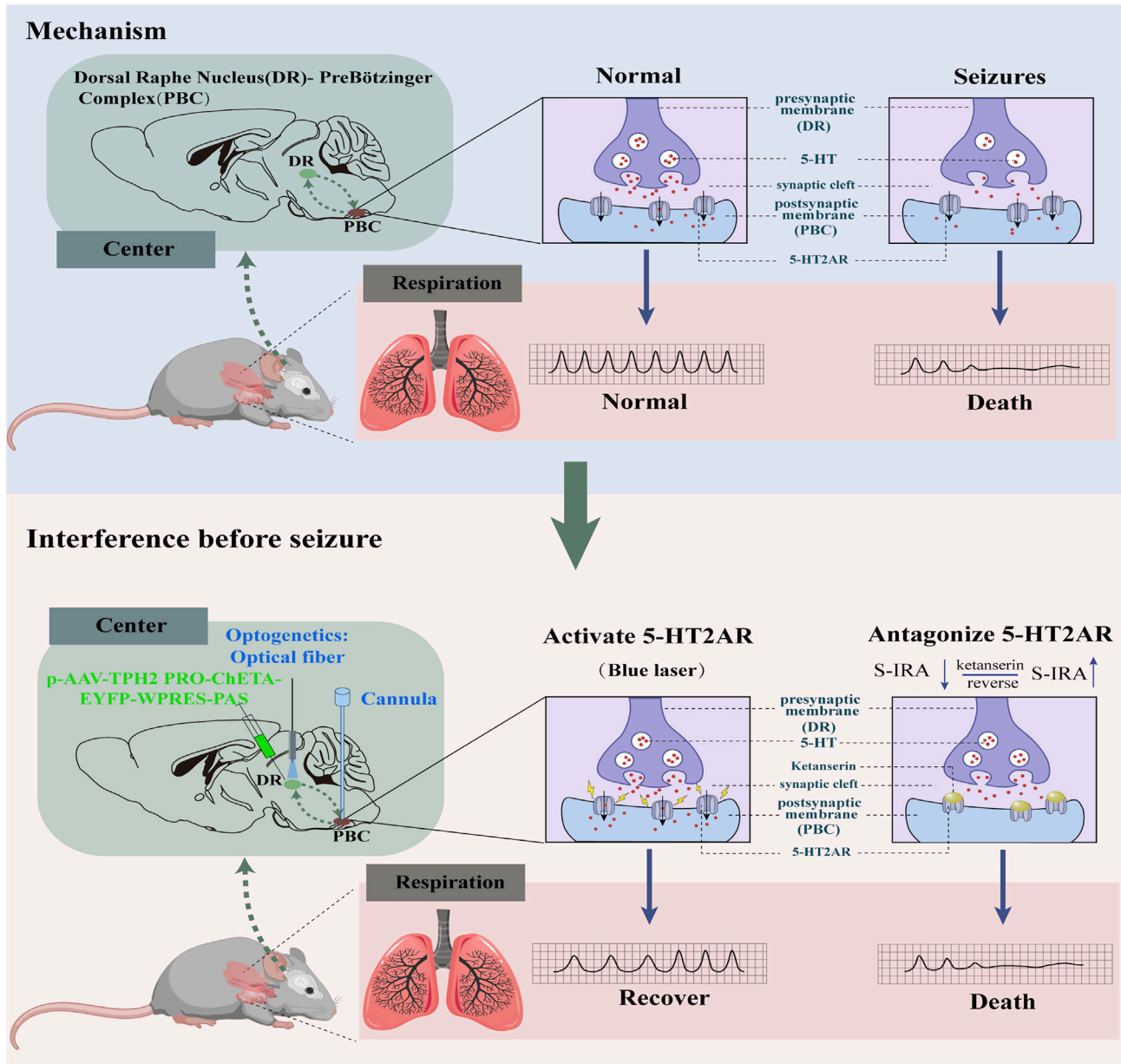


Figure 13. Mechanism by which 5-HT neurons in the brain modulate S-IRA and SUDEP via the neural circuit between DR and PBC
SUDEP, sudden unexpected death in epilepsy; S-IRA, seizure-induced respiratory arrest; KET, ketanserin; PBC, pre-Bötzinger complex; DR, dorsal raphe nucleus; 5-HT2AR, 5-HT2A receptor.

circuit between the DR and PBC is implicated in S-IRA induced by seizures. Therefore, 5-HT2AR in the PBC may be a specific and key target for the development of interventions to prevent SUDEP (Figure 13).

Limitations of the study

This study also has some limitations. We suggested that the serotonergic neural circuit between the DR and PBC is a major cause of S-IRA induced by seizures. To further examine the bridge between the DR and PBC and its role in modulating S-IRA in our models, we used CTB-555, a nerve retrograde tracer, to confirm and establish the neural circuit between the DR and PBC. However, there is insufficient evidence for the specificity of DR 5-HT neuronal manipulations and retrograde prediction between DR and PBC. When CTB-555 was

injected into DR, it showed up in the PBC and vice versa, but these manifestations emerged one week after the CTB injection, suggesting that this approach may not be the most effective for proving the existence of direct synaptic connections between the DR and PBC. Furthermore, activation of *c-fos* in PBC with DR optogenetic stimulation may not be a direct way to validate the projection between these two nuclei. In the future, we will employ specific methods, using tracers other than CTB-555, to trace and investigate the neuronal circuit between DR and PBC as well as the direct synaptic connections from 5-HT neurons of DR to PBC.

STAR★METHODS

Detailed methods are provided in the online version of this paper and include the following:

- KEY RESOURCES TABLE
- RESOURCE AVAILABILITY
 - Lead contact
 - Materials availability
 - Data and code availability
- EXPERIMENTAL MODEL AND SUBJECT DETAILS
 - Animals
 - Seizure induction and resuscitation
- METHOD DETAILS
 - Pharmacology experiment
 - Optogenetics experiments
 - Photostimulation of the DR-mediated suppression of S-IRA by PTZ and on EEG changes
- QUANTIFICATION AND STATISTICAL ANALYSIS

SUPPLEMENTAL INFORMATION

Supplemental information can be found online at <https://doi.org/10.1016/j.isci.2022.105228>.

ACKNOWLEDGMENTS

The work was supported by the National Natural Science Foundation of China (Grant.NO: 81771403, 81974205); by the Natural Science Foundation of Zhejiang Province (LZ20H090001); by the Program of New Century 131 outstanding young talent plan top-level of Hang Zhou to HHZ; and by the National Natural Science Foundation of China (Grant.NO: 81771138) to Han Lu and by the National Natural Science Foundation of China (Grant.NO: 82001379) and the Natural Science Foundation of Hunan Province (Grant.NO: 2020JJ5952) to HTZ; Nature Science Foundation of Hunan Province, China (No. 2021JJ31047) to CZ. We are grateful to YuDong Zhou and Yi Shen for the experimental design.

AUTHOR CONTRIBUTION

HHZ designed the study. HHZ. wrote the article. HXM, QY, YS, XTL, LYG. performed and analyzed most of the experiments. YL W, QX, HL, HTZ, and C Z helped with the analysis of experiments. Kazuki Nagayasu contributed intellectually to the article concerning the Plasmid design for TPH2-CheTA.

DECLARATION OF INTERESTS

All authors declare no competing interests.

Received: March 28, 2022

Revised: August 14, 2022

Accepted: September 23, 2022

Published: October 21, 2022

REFERENCES

- Aghajanian, G.K., and Marek, G.J. (1999). Serotonin, via 5-HT_{2A} receptors, increases EPSCs in layer V pyramidal cells of prefrontal cortex by an asynchronous mode of glutamate release. *Brain Res.* 825, 161–171. [https://doi.org/10.1016/S0006-8993\(99\)01224-x](https://doi.org/10.1016/S0006-8993(99)01224-x).
- Alheid, G.F., Gray, P.A., Jiang, M.C., Feldman, J.L., and McCrimmon, D.R. (2002). Parvalbumin in respiratory neurons of the ventrolateral medulla of the adult rat. *J. Neurocytol.* 31, 693–717. <https://doi.org/10.1023/a:1025799830302>.
- Andalman, A.S., Burns, V.M., Lovett-Barron, M., Broxton, M., Poole, B., Yang, S.J., Grosenick, L., Lerner, T.N., Chen, R., Benster, T., et al. (2019). Neuronal dynamics regulating brain and behavioral state transitions. *Cell* 177, 970–985.e20. <https://doi.org/10.1016/j.cell.2019.02.037>.

- Aznar, S., and Hervig, M.E.-S. (2016). The 5-HT2A serotonin receptor in executive function: implications for neuropsychiatric and neurodegenerative diseases. *Neurosci. Biobehav. Rev.* *64*, 63–82. <https://doi.org/10.1016/j.neubiorev.2016.02.008>.
- Bateman, L.M., Li, C.-S., Lin, T.-C., and Seyal, M. (2010a). Serotonin reuptake inhibitors are associated with reduced severity of ictal hypoxemia in medically refractory partial epilepsy. *Epilepsia* *51*, 2211–2214. <https://doi.org/10.1111/j.1528-1167.2010.02594.x>.
- Bateman, L.M., Li, C.-S., and Seyal, M. (2008). Ictal hypoxemia in localization-related epilepsy: analysis of incidence, severity and risk factors. *Brain* *131*, 3239–3245. <https://doi.org/10.1093/brain/awn277>.
- Bateman, L.M., Spitz, M., and Seyal, M. (2010b). Ictal hypoventilation contributes to cardiac arrhythmia and SUDEP: report on two deaths in video-EEG-monitored patients. *Epilepsia* *51*, 916–920. <https://doi.org/10.1111/j.1528-1167.2009.02513.x>.
- Buchanan, G.F., Murray, N.M., Hajek, M.A., and Richerson, G.B. (2014). Serotonin neurones have anti-convulsant effects and reduce seizure-induced mortality. *J. Physiol.* *592*, 4395–4410. <https://doi.org/10.1113/jphysiol.2014.277574>.
- Chen, Q., Tian, F., Yue, Q., Zhan, Q., Wang, M., Xiao, B., and Zeng, C. (2019). Decreased serotonin synthesis is involved in seizure-induced respiratory arrest in DBA/1 mice. *Neuroreport* *30*, 842–846. <https://doi.org/10.1097/WNR.0000000000001287>.
- Cheng, H., Qi, Y., Lai, N., Yang, L., Xu, C., Wang, S., Guo, Y., Chen, Z., and Wang, Y. (2021). Inhibition of hyperactivity of the dorsal raphe 5-HTergic neurons ameliorates hippocampal seizure. *CNS Neurosci. Ther.* *27*, 963–972. <https://doi.org/10.1111/cns.13648>.
- Damasceno, D.D., Savergnini, S.Q., Gomes, E.R.M., Guatimosim, S., Ferreira, A.J., Doretto, M.C., and Almeida, A.P. (2013). Cardiac dysfunction in rats prone to audiogenic epileptic seizures. *Seizure* *22*, 259–266. <https://doi.org/10.1016/j.seizure.2013.01.006>.
- Devinsky, O., Hesdorffer, D.C., Thurman, D.J., Lhatoo, S., and Richerson, G. (2016). Sudden unexpected death in epilepsy: epidemiology, mechanisms, and prevention. *Lancet Neurol.* *15*, 1075–1088. [https://doi.org/10.1016/S1474-4422\(16\)30158-2](https://doi.org/10.1016/S1474-4422(16)30158-2).
- Donato Di Paola, E., Gareri, P., Davoli, A., Gratteri, S., Scicchitano, F., Naccari, C., and De Sarro, G. (2007). Influence of levetiracetam on the anticonvulsant efficacy of conventional antiepileptic drugs against audiogenic seizures in DBA/2 mice. *Epilepsia Res.* *75*, 112–121. <https://doi.org/10.1016/j.eplepsyres.2007.04.008>.
- Faingold, C.L., Randall, M., Mhaskar, Y., and Uteshev, V.V. (2011). Differences in serotonin receptor expression in the brainstem may explain the differential ability of a serotonin agonist to block seizure-induced sudden death in DBA/2 vs. DBA/1 mice. *Brain Res.* *1418*, 104–110. <https://doi.org/10.1016/j.brainres.2011.08.043>.
- Faingold, C.L., and Randall, M. (2013). Effects of age, sex, and sertraline administration on seizure-induced respiratory arrest in the DBA/1 mouse model of sudden unexpected death in epilepsy (SUDEP). *Epilepsy Behav.* *28*, 78–82. <https://doi.org/10.1016/j.yebeh.2013.04.003>.
- García-Oscos, F., Torres-Ramírez, O., Dinh, L., Galindo-Charles, L., Pérez Padilla, E.A., Pineda, J.C., Atzori, M., and Salgado, H. (2015). Activation of 5-HT receptors inhibits GABAergic transmission by pre- and post-synaptic mechanisms in layer II/III of the juvenile rat auditory cortex. *Synapse* *69*, 115–127. <https://doi.org/10.1002/syn.21794>.
- Gewirtz, J.C., and Marek, G.J. (2000). Behavioral evidence for interactions between a hallucinogenic drug and group II metabotropic glutamate receptors. *Neuropsychopharmacology* *23*, 569–576. [https://doi.org/10.1016/S0893-133X\(00\)00136-6](https://doi.org/10.1016/S0893-133X(00)00136-6).
- Hegerl, U., and Juckel, G. (1993). Intensity dependence of auditory evoked potentials as an indicator of central serotonergic neurotransmission: a new hypothesis. *Biol. Psychiatry* *33*, 173–187. [https://doi.org/10.1016/0006-3223\(93\)90137-3](https://doi.org/10.1016/0006-3223(93)90137-3).
- Juckel, G., Pogarell, O., Augustin, H., Mulert, C., Müller-Siecheneder, F., Frodl, T., Mavrogiorgou, P., and Hegerl, U. (2007). Differential prediction of first clinical response to serotonergic and noradrenergic antidepressants using the loudness dependence of auditory evoked potentials in patients with major depressive disorder. *J. Clin. Psychiatry* *68*, 1206–1212. <https://doi.org/10.4088/jcp.v68n0806>.
- Kähkönen, S., Jääskeläinen, I.P., Pennanen, S., Liesivuori, J., and Ahveninen, J. (2002). Acute tryptophan depletion decreases intensity dependence of auditory evoked magnetic N1/P2 dipole source activity. *Psychopharmacology (Berl)* *164*, 221–227. <https://doi.org/10.1007/s00213-002-1194-z>.
- Kawashima, T., Zwart, M.F., Yang, C.-T., Mense, B.D., and Ahrens, M.B. (2016). The serotonergic system tracks the outcomes of actions to mediate short-term motor learning. *Cell* *167*, 933–946.e20. <https://doi.org/10.1016/j.cell.2016.09.055>.
- Kulikov, A.V., Osipova, D.V., Naumenko, V.S., and Popova, N.K. (2005). Association between Tph2 gene polymorphism, brain tryptophan hydroxylase activity and aggressiveness in mouse strains. *Genes Brain Behav.* *4*, 482–485. <https://doi.org/10.1111/j.1601-183X.2005.00145.x>.
- Lalley, P.M., Bischoff, A.M., and Richter, D.W. (1994). Serotonin 1A-receptor activation suppresses respiratory apneusis in the cat. *Neurosci. Lett.* *172*, 59–62. [https://doi.org/10.1016/0304-3940\(94\)90666-2](https://doi.org/10.1016/0304-3940(94)90666-2).
- Lhatoo, S., Noebels, J.E., and Whittemore, V.; NINDS Center for SUDEP Research (2015). Sudden unexpected death in epilepsy: identifying risk and preventing mortality. *Epilepsia* *56*, 1700–1706. <https://doi.org/10.1111/epi.13134>.
- Marek, G.J., Wright, R.A., Schoepp, D.D., Monn, J.A., and Aghajanian, G.K. (2000). Physiological antagonism between 5-hydroxytryptamine(2A) and group II metabotropic glutamate receptors in prefrontal cortex. *J. Pharmacol. Exp. Ther.* *292*, 76–87.
- Massey, C.A., Sowers, L.P., Dlouhy, B.J., and Richerson, G.B. (2014). Mechanisms of sudden unexpected death in epilepsy: the pathway to prevention. *Nat. Rev. Neurol.* *10*, 271–282. <https://doi.org/10.1038/nrneurol.2014.64>.
- Mengod, G., Palacios, J.M., and Cortés, R. (2015). Cartography of 5-HT1A and 5-HT2A receptor subtypes in prefrontal cortex and its projections. *ACS Chem. Neurosci.* *6*, 1089–1098. <https://doi.org/10.1021/acscchemneuro.5b00023>.
- Morinaga, R., Nakamura, N., and Yamamoto, Y. (2019). Serotonergic projections to the ventral respiratory column from raphe nuclei in rats. *Neurosci. Res.* *143*, 20–30. <https://doi.org/10.1016/j.neures.2018.05.004>.
- Nagai, Y., Takayama, K., Nishitani, N., Andoh, C., Koda, M., Shirakawa, H., Nakagawa, T., Nagayasu, K., Yamanaka, A., and Kaneko, S. (2020). The role of dorsal raphe serotonin neurons in the balance between reward and aversion. *Int. J. Mol. Sci.* *21*, E2160. <https://doi.org/10.3390/ijms21062160>.
- Nathan, P.J., Segrave, R., Phan, K.L., O'Neill, B., and Croft, R.J. (2006). Direct evidence that acutely enhancing serotonin with the selective serotonin reuptake inhibitor citalopram modulates the loudness dependence of the auditory evoked potential (LDAEP) marker of central serotonin function. *Hum. Psychopharmacol.* *21*, 47–52. <https://doi.org/10.1002/hup.740>.
- Osipova, D.V., Kulikov, A.V., Mekada, K., Yoshiki, A., Moshkin, M.P., Kotenkova, E.V., and Popova, N.K. (2010). Distribution of the C1473G polymorphism in tryptophan hydroxylase 2 gene in laboratory and wild mice. *Genes Brain Behav.* *9*, 537–543. <https://doi.org/10.1111/j.1601-183X.2010.00586.x>.
- Ozawa, Y., and Okado, N. (2002). Alteration of serotonergic receptors in the brain stems of human patients with respiratory disorders. *Neuropediatrics* *33*, 142–149. <https://doi.org/10.1055/s-2002-33678>.
- Peña, F., and Ramirez, J.-M. (2002). Endogenous activation of serotonin-2A receptors is required for respiratory rhythm generation in vitro. *J. Neurosci.* *22*, 11055–11064.
- Ptak, K., Yamanishi, T., Aungst, J., Milescu, L.S., Zhang, R., Richerson, G.B., and Smith, J.C. (2009). Raphé neurons stimulate respiratory circuit activity by multiple mechanisms via endogenously released serotonin and substance P. *J. Neurosci.* *29*, 3720–3737. <https://doi.org/10.1523/JNEUROSCI.5271-08.2009>.
- Rao, D., Basura, G.J., Roche, J., Daniels, S., Mancilla, J.G., and Manis, P.B. (2010). Hearing loss alters serotonergic modulation of intrinsic excitability in auditory cortex. *J. Neurophysiol.* *104*, 2693–2703. <https://doi.org/10.1152/jn.01092.2009>.
- Ren, J., Isakova, A., Friedmann, D., Zeng, J., Grutzner, S.M., Pun, A., Zhao, G.Q., Kolluru, S.S., Wang, R., Lin, R., et al. (2019). Single-cell transcriptomes and whole-brain projections of serotonin neurons in the mouse dorsal and

median raphe nuclei. *Elife* 8, e49424. <https://doi.org/10.7554/eLife.49424>.

Richter, D.W., Manzke, T., Wilken, B., and Ponimaskin, E. (2003). Serotonin receptors: guardians of stable breathing. *Trends Mol. Med.* 9, 542–548. <https://doi.org/10.1016/j.molmed.2003.10.010>.

Ryvlin, P., Nashef, L., Lhatoo, S.D., Bateman, L.M., Bird, J., Bleasel, A., Boon, P., Crespel, A., Dworetzky, B.A., Høgenhaven, H., et al. (2013). Incidence and mechanisms of cardiorespiratory arrests in epilepsy monitoring units (MORTEMUS): a retrospective study. *Lancet Neurol.* 12, 966–977. [https://doi.org/10.1016/S1474-4422\(13\)70214-X](https://doi.org/10.1016/S1474-4422(13)70214-X).

Schwarzacher, S.W., Pestean, A., Günther, S., and Ballanyi, K. (2002). Serotonergic modulation of respiratory motoneurons and interneurons in brainstem slices of perinatal rats. *Neuroscience* 115, 1247–1259. [https://doi.org/10.1016/s0306-4522\(02\)00540-7](https://doi.org/10.1016/s0306-4522(02)00540-7).

Shen, Y., Ma, H.X., Lu, H., Zhao, H.T., Sun, J.L., Cheng, Y., and Zhang, H.H. (2021). Central deficiency of norepinephrine synthesis and norepinephrine neurotransmission contributes to seizure-induced respiratory arrest. *Biomed. Pharmacother.* 133, 111024. <https://doi.org/10.1016/j.biopha.2020.111024>.

Smith, J.C., Abdala, A.P.L., Rybak, I.A., and Paton, J.F.R. (2009). Structural and functional

architecture of respiratory networks in the mammalian brainstem. *Philos. Trans. R. Soc. Lond. B Biol. Sci.* 364, 2577–2587. <https://doi.org/10.1098/rstb.2009.0081>.

Tryba, A.K., Peña, F., and Ramirez, J.-M. (2006). Gasping activity in vitro: a rhythm dependent on 5-HT_{2A} receptors. *J. Neurosci.* 26, 2623–2634. <https://doi.org/10.1523/JNEUROSCI.4186-05.2006>.

Vilella, L., Lacuey, N., Hampson, J.P., Rani, M.R.S., Sainju, R.K., Friedman, D., Nei, M., Strohl, K., Scott, C., Gehlbach, B.K., et al. (2019). Postconvulsive central apnea as a biomarker for sudden unexpected death in epilepsy (SUDEP). *Neurology* 92, e171–e182. <https://doi.org/10.1212/WNL.0000000000006785>.

Wutzler, A., Winter, C., Kitzrow, W., Uhl, I., Wolf, R.J., Heinz, A., and Juckel, G. (2008). Loudness dependence of auditory evoked potentials as indicator of central serotonergic neurotransmission: simultaneous electrophysiological recordings and in vivo microdialysis in the rat primary auditory cortex. *Neuropsychopharmacology* 33, 3176–3181. <https://doi.org/10.1038/npp.2008.42>.

Zeng, C., Long, X., Cotten, J.F., Forman, S.A., Solt, K., Faingold, C.L., and Feng, H.-J. (2015). Fluoxetine prevents respiratory arrest without enhancing ventilation in DBA/1 mice. *Epilepsy Behav.* 45, 1–7. <https://doi.org/10.1016/j.yebeh.2015.02.013>.

Zhang, H., Zhao, H., and Feng, H.-J. (2017). Atomoxetine, a norepinephrine reuptake inhibitor, reduces seizure-induced respiratory arrest. *Epilepsy Behav.* 73, 6–9. <https://doi.org/10.1016/j.yebeh.2017.04.046>.

Zhang, H., Zhao, H., Yang, X., Xue, Q., Cotten, J.F., and Feng, H.-J. (2016). 5-Hydroxytryptophan, a precursor for serotonin synthesis, reduces seizure-induced respiratory arrest. *Epilepsia* 57, 1228–1235. <https://doi.org/10.1111/epi.13430>.

Zhang, H., Zhao, H., Zeng, C., Van Dort, C., Faingold, C.L., Taylor, N.E., Solt, K., and Feng, H.-J. (2018). Optogenetic activation of 5-HT neurons in the dorsal raphe suppresses seizure-induced respiratory arrest and produces anticonvulsant effect in the DBA/1 mouse SUDEP model. *Neurobiol. Dis.* 110, 47–58. <https://doi.org/10.1016/j.nbd.2017.11.003>.

Zhao, H., Cotten, J.F., Long, X., and Feng, H.-J. (2017). The effect of atomoxetine, a selective norepinephrine reuptake inhibitor, on respiratory arrest and cardiorespiratory function in the DBA/1 mouse model of SUDEP. *Epilepsy Res.* 137, 139–144. <https://doi.org/10.1016/j.eplepsyres.2017.08.005>.

Zhao, H., Zhang, H., Schoen, F.J., Schachter, S.C., and Feng, H.-J. (2019). Repeated generalized seizures can produce calcified cardiac lesions in DBA/1 mice. *Epilepsy Behav.* 95, 169–174. <https://doi.org/10.1016/j.yebeh.2019.04.010>.

STAR★METHODS

KEY RESOURCES TABLE

REAGENT or RESOURCE	SOURCE	IDENTIFIER
Antibodies		
Rabbit anti-c-fos primary antibody	Cell Signaling Technology	2250T
Mouse anti-TPH2 primary antibody	Sigma-Aldrich	T0678
Donkey anti-mouse Alexa 488	Thermo Fisher Scientific	A32766
Donkey anti-mouse Alexa 546	Thermo Fisher Scientific	A10036
Goat anti-rabbit cy5	Thermo Fisher Scientific	A10523
Goat anti-mouse cy5	Thermo Fisher Scientific	A10524
Rabbit anti-NK1	Sigma-Aldrich	SAB4502913
Mouse anti-SA-2AR	Santa Cruz Biotechnology	sc-166775
Anti-rabbit Alexa 488 secondary antibody	Thermo Fisher Scientific	A32766
Bacterial and virus strains		
pAAV-TPH2 PRO-ChETA-EYFP-WPRES-PAS	Sheng BO, Co., Ltd.	N/A
AAV2/9-mCaMKIIa-GCaMP6f-WPRE-pA	Taitool Bioscience Co., Ltd.	N/A
Chemicals, peptides, and recombinant proteins		
PTZ	Sigma-Aldrich, St. Louis, MO	Cat #P6500
KET	Sigma-Aldrich	Cat #8006
5-HTP	Sigma-Aldrich	Cat #107751
CTB-555	BrainVTA Technology Co. Ltd	N/A
Experimental models: Organisms/strains		
DBA/1 mice	the Animal Center of Zhejiang University School of Medicine	N/A
Software and algorithms		
ImageJ	NIH, Bethesda, MD, USA	https://imagej.nih.gov/ij/

RESOURCE AVAILABILITY

Lead contact

Further information and requests should be directed to and will be fulfilled by the lead contact, Honghai Zhang (zhanghonghai_0902@163.com).

Materials availability

This study did not generate new unique reagents.

Data and code availability

- All data reported in this paper will be shared by the [lead contact](#) upon request.
- No original code was reported in this study.
- Additional information related to this study is available from the [lead contact](#) upon request.

EXPERIMENTAL MODEL AND SUBJECT DETAILS

Animals

All experimental procedures were in line with the National Institutes of Health Guidelines for the Care and Use of Laboratory Animals and approved by the Animal Advisory Committee of Zhejiang University. DBA/1 mice were housed and bred in the Animal Center of Zhejiang University School of Medicine and given

rodent food and water *ad libitum*. DBA/1 mice of either gender were used in the experiments, as previous study suggested that gender is not a variable affecting S-IRA in DBA/1 mice (Faingold and Randall, 2013). For the acoustic stimulation murine model, DBA/1 mice were “primed” starting from postnatal days 26–28 to establish consistent susceptibility to audiogenic seizures and S-IRA. For the PTZ-evoked seizure model, PTZ was administered to non-primed DBA/1 mice at approximately 8 weeks of age (Shen et al., 2021). TPH2-ChETA (E123 T mutation in Channelrhodopsin 2 [*ChR2*])–expressing mice were generated by viral delivery of pAAV-TPH2 PRO-ChETA-EYFP-WPRES-PAS under the control of the promoter of TPH2 into the DR, and after 3 weeks, TPH2-ChETA expression in the DR was confirmed by immunohistochemistry upon completion of optogenetics experiments. The promoter for TPH2 that we used in the present study has been used previously to infect 5-HT neurons in the DR by our group to modulate the balance between reward and aversion (Nagai et al., 2020).

Seizure induction and resuscitation

S-IRA was evoked by acoustic stimulation or intraperitoneal (IP) administration of PTZ, as previously described (Chen et al., 2019; Vilella et al., 2019; Zeng et al., 2015; Zhang et al., 2017, 2018; Zhao et al., 2017). For the acoustic stimulation model, each mouse was placed in a cylindrical plexiglass chamber in a sound-isolated room, and AGSz were evoked by an electric bell (96 dB SPL, Zhejiang People’s Electronics, China). Acoustic stimulation was given for a maximum duration of 60 s or until the onset of tonic seizures and S-IRA. For the PTZ-evoked seizure model, S-IRA was evoked in non-primed DBA/1 mice by IP administration of a single dose of PTZ (Cat #P6500; Sigma-Aldrich, St. Louis, MO) at a dose of 75 mg/kg. Mice with S-IRA were resuscitated within 5 s after the final respiratory gasp using a rodent respirator (YuYan Instruments, Shanghai, China).

METHOD DETAILS

Pharmacology experiment

Effect of IP administration of KET on 5-HTP-mediated suppression of S-IRA evoked by acoustic stimulation

As shown in Figure 1A, susceptibility to S-IRA in primed DBA/1 mice was confirmed 24 h prior to treatment with 5-HTP (Cat #107751; Sigma-Aldrich) or vehicle. 5-HTP (200 mg/kg) or vehicle (saline) was administered IP once daily for 2 days, and induction of S-IRA was performed 75 min after the second administration. KET (Cat #8006; Sigma-Aldrich) at different doses or vehicle (25% dimethyl sulfoxide [DMSO]) was administered IP 15 min before acoustic stimulation. The incidence of S-IRA, latency to AGSz, duration of wild running and clonic seizures, duration of tonic-clonic seizures, and seizure scores were determined by offline analysis of video recordings (Bateman et al., 2010a; Ozawa and Okado, 2002; Vilella et al., 2019; Zhang et al., 2016, 2018, 2017; Zhao et al., 2017, 2019).

Effect of ICV administration of KET on 5-HTP-mediated suppression of S-IRA by PTZ

For intracerebroventricular (ICV) injection, an ICV guide cannula (O.D.1.41 × I.D.0.25mm/M3.5, 62,004, RWD Life Science Inc., China) was implanted into the right lateral ventricle (AP - 0.45 mm; ML - 1.0 mm; V - 2.50 mm) to enable microinjections as previously described (Chen et al., 2019; Zhang et al., 2017). DBA/1 mice were given 5-HTP or vehicle (saline) in the same manner prior to PTZ IP injection, and KET or vehicle (25% DMSO) was administered by ICV injection 15 min after (Figure 2A). The incidence of S-IRA, latency to AGSz, duration of wild running and clonic seizures, duration of tonic-clonic seizures, and seizure scores were determined by offline analysis of video recordings (Bateman et al., 2010a; Ozawa and Okado, 2002; Vilella et al., 2019; Zhang et al., 2016, 2018, 2017; Zhao et al., 2017, 2019). The video recordings would last 1 h after PTZ administration. The group treatments were as follows: 1) saline (IP) was administered 75 min prior to PTZ (75 mg/kg, IP) and 25% DMSO (2 μ L, at a rate of 0.5 μ L/min ICV) 15 min prior to PTZ injection as control; 2) 5-HTP (200 mg/kg, IP) was administered 75 min prior to PTZ (75 mg/kg, IP) and 25% DMSO (2 μ L, at a rate of 0.5 μ L/min ICV) 15 min prior to PTZ injection; and 3) 5-HTP (200 mg/kg, IP) was administered 75 min prior to PTZ (75 mg/kg, IP), with KET (9.15 nmol or 18.3 nmol, dissolved in 2 μ L 25% DMSO, at a rate of 0.5 μ L/min ICV) administered 15 min prior to PTZ injection.

Effect of PBC microinjection of KET on 5-HTP-mediated suppression of S-IRA by PTZ

For microinjection of KET in the bilateral PBC, guide cannulas (O.D.0.48 × I.D.0.34 mm/M3.5,62,033, RWD Life Science Inc.) were implanted on both sides. One week after the operation, the experiment was carried

out, with microinjection of KET(200 nL, 10 mg/mL) into every unilateral PBC to observe whether the mice died in 24 h. 5-HTP (200 mg/kg) or vehicle (saline) was administered IP once daily for 2 days. Microinjection of KET (200 nL, 10 mg/mL) into every unilateral PBC is performed 10mins before IP PTZ. Induction of S-IRA was performed 70 min after the 5-HTP second administration.

Optogenetics experiments

Stereotactic surgery

DBA/1 mice at 8 weeks of age were anesthetized with 3.5% chloral hydrate and head-fixed in a stereotaxic apparatus (68,018, RWD Life Science Inc., Shenzhen, China), as previously described (Zhang et al., 2018). Throughout the entire surgical process, the body temperature of anesthetized mice was kept constant at 37°C using a heating pad. If the DBA/1 mice showed pain in response to a paw pinch, an additional 10% of the initial dosage of sodium pentobarbital was given to guarantee a painless state. For optogenetic viral delivery of pAAV-TPH2 PRO-ChETA-EYFP-WPRES-PAS, microinjection (100 nL, at a rate of 40 nL/min) was performed using the following stereotaxic coordinates for the DR (AP – 4.55 mm, ML – 0.44 mm, DV – 2.80 mm, 10°right) based on the mouse brain atlas. Viruses were delivered via a gauge needle for the specification of 10ul (cat# 60700010, Gao Ge, Co., Ltd, ShangHai, China) by an Ultra Micro Pump (160494 F10E, WPI) over a period of 10 min(including the residence time of the needle tip in the brain area before and after injection); the syringe was not removed until 15–20 min after the end of infusion to allow diffusion of the viruses. Then, the optical fiber (FOC-W-1.25-200-0.37-3.0, Inper, Hangzhou, China) was implanted above the area (AP – 4.55 mm, ML – 0.44 mm, DV – 2.80 mm, 10°right) for 0.05 mm(AP – 4.55 mm, ML – 0.44 mm, DV – 2.75 mm, 10°right). For ICV surgery, ICV guide cannula implantation was completed as described for the pharmacology experiment and was implanted with a headstage for EEG in the same mice as previously described (Chen et al., 2019). For microinjection of KET in the bilateral PBC, guide cannulas (O.D.0.48 × I.D.0.34 mm/M3.5,62033, RWD Life Science Inc.) were implanted on both sides. CTB-555 (100 nL, 1 μg/μL, BrainVTA Technology Co. Ltd, Wuhan, China) was injected in the DR (AP – 4.55 mm, ML – 0.44 mm, DV – 2.80 mm, 10°right) or the right side of the PBC (AP – 6.80 mm, ML – 1.25 mm, DV – 4.95 mm), and we waited approximately 1 week for retrograde labeling of projection neurons. For the photostimulation of the bilateral PBC, pAAV-TPH2 PRO-ChETA-EYFP-WPRES-PAS was delivered in the bilateral PBC (AP – 6.80 mm, ML – 1.25 mm, DV – 4.95 mm) based on the mouse brain atlas 3 weeks before the experiments, and an optical fiber within a guide cannula (O.D.0.48 × I.D.0.34mm/M3.5, 62,033, RWD Life and FOC-W-1.25-200-0.37-3.0, Inper, Hangzhou, China) over 0.05 mm was implanted. For the photometry recordings, viral delivery of AAV2/9-mCaMKIIa-GCaMP6f-WPRE-pA via microinjection (100 nL, at a rate of 40 nL/min) was performed using the following stereotaxic coordinates for the bilateral PBC (AP – 6.80 mm, ML – 1.25 mm, DV – 4.95 mm) based on the mouse brain atlas 3 weeks before the experiments, and an optical fiber (FOC-W-1.25-200-0.37-3.0, Inper) over 0.05 mm was implanted.

Fiber photometry

Three weeks after the injection of the virus, the group that DR infected with ChETA and GCaMP6f in the bilateral PBC was established. The fiber photometry system (Inper, Hangzhou, China, C11946) used a 488-nm diode laser. The recording was started 20 min before IP injection of PTZ (75 mg/kg) and stopped 20 min after PTZ injection. Data for the individual trials of clonic seizures and tonic seizures were derived from a heatmap and the change in fluorescence values ($\Delta F/F$) was calculated as $(F - F_0)/F_0$.

Photostimulation of the DR-mediated suppression of S-IRA by PTZ and on EEG changes

pAAV-TPH2 PRO-ChETA-EYFP-WPRES-PAS was delivered into the DR of DBA/1 mice 3 weeks before experiments, and an ICV guide cannula with a headstage for EEG was implanted. The DBA/1 mice were divided into three groups. For the control group without photostimulation of the DR ($n = 7$), ICV injection of vehicle (25% DMSO, 2 μL) was given in a uniform manner at the manner (0.5 μL/min) 30 min prior to IP injection of PTZ (75 mg/kg). For the group treated with photostimulation of the DR without ICV delivery of KET ($n = 6$), ICV injection of the same concentration and volume of vehicle (25% DMSO, 2 μL) was given 15 min prior to photostimulation and 30 min prior to IP injection of PTZ (75 mg/kg). For another group treated with photostimulation of the DR and ICV delivery of KET ($n = 7$), ICV injection of KET (total dose, 18.3 nmol) was given 15 min prior to photostimulation and 30 min prior to IP injection of PTZ (75 mg/kg). The incidence of S-IRA, latency to AGSs, duration of wild running and clonic seizures, duration of tonic-clonic seizures, and seizure scores in each group were analyzed statistically. EEG recordings in the three groups were started 25 min before PTZ injection and ended 20 min after PTZ injection. EEG activity was

statistically analyzed as previously described (Chen et al., 2019). The parameters for photostimulation of the DR were: blue-light, 465 nm, 20 Hz, 20-ms pulse width, 15 mW, and 20 min) was delivered by the laser (B12124, Inper) through a 200- μ m optic fiber, which was proved to be effective on the suppression of S-IRA (Zhang et al., 2018).

Photometric analysis of DR-mediated suppression of S-IRA by PTZ after microinjection of KET in the bilateral PBC

pAAV-TPH2 PRO-ChETA-EYFP-WPRES-PAS was delivered into the DR of DBA/1 mice 3 weeks before experiments, and guide cannulas (62,033, RWD Life Science 1 Inc., China) were implanted in the bilateral PBC. For the control group treated without photostimulation of the DR and administration of KET, microinjection of the vehicle (25% DMSO, 2 μ L) into the bilateral PBC was given in a uniform manner (0.5 μ L/min) 25 min prior to IP injection of PTZ (75 mg/kg). For the group treated with photostimulation of the DR without administration of KET (n = 7), microinjection of the vehicle (25% DMSO) into the bilateral PBC was given in a uniform manner (0.5 μ L/min) 25 min prior to IP injection of PTZ (75 mg/kg). For another group treated with photostimulation of the DR and administration of KET (n = 7), microinjection of KET with 200 nL (containing 4 μ g KET) into every unilateral PBC was given 25 min prior to IP injection of PTZ (75 mg/kg). Both groups received laser stimulation 10 min after microinjection. KET (8 μ g in 400 nL) was given per mouse in the bilateral PBC. The parameters for photostimulation of the DR were the same as in the ICV experiments.

Photometric analysis of the incidence of PTZ-induced S-IRA with TPH2-ChETA infection of neurons of the bilateral PBC and microinjection of KET in the bilateral PBC

DBA/1 mice were used 3 weeks after viral delivery of pAAV-TPH2 PRO-ChETA-EYFP-WPRES-PAS into the bilateral PBC. For the control group treated without photostimulation (n = 6), microinjection of the vehicle (25% DMSO, 2 μ L) into every unilateral PBC was given in a uniform manner (0.5 μ L/min) 25 min prior to IP injection of PTZ (75 mg/kg). For the experimental group treated with photostimulation of the bilateral PBC (n = 7), microinjection of the same concentration and volume of vehicle (25% DMSO) into every unilateral PBC was given 25 min prior to IP injection of PTZ (75 mg/kg). For the group treated with KET and photostimulation of the bilateral PBC (n = 3), microinjection of KET (4 μ g, 200 nL) into every unilateral PBC was given 25 min prior to IP injection of PTZ (75 mg/kg). The parameters for photostimulation of the bilateral PBC were: blue-light, 465 nm, 20 Hz, 20-ms pulse width, 15 mW, and 20 min.

Photometric analysis of Ca²⁺ activity of neurons in the bilateral PBC with photo-stimulation of TPH2-ChETA neurons in the DR in PTZ-induced S-IRA model

DBA/1 mice were used 3 weeks after viral delivery of pAAV-TPH2 PRO-ChETA-EYFP-WPRES-PAS or AAV2/9-mCaMKIIa-GCaMP6f-WPRE-pA (100 nL, at a rate of 40 nL/min) into the DR and the bilateral PBC. For the control group treated with pAAV-TPH2 PRO-ChETA-EYFP-WPRES-PAS in the DR without photostimulation and AAV2/9-mCaMKIIa-GCaMP6f-WPRE-pA in the bilateral PBC (n = 3), photometry recordings were started 20 min prior to IP injection of PTZ (75 mg/kg) and ended 40 min after PTZ injection or until the death of mice if within 60 min. For the group treated with pAAV-TPH2 PRO-ChETA-EYFP-WPRES-PAS in the DR and photostimulation of the DR as well as AAV2/9-mCaMKIIa-GCaMP6f-WPRE-pA in the bilateral PBC (n = 3), photometry recordings were started 20 min prior to IP injection of PTZ (75 mg/kg) and ended 40 min after PTZ injection or until the death of mice if within 60 min. The fiber photometry system (Inper, C11946) used a 488-nm diode laser. We segmented the data based on individual trials of seizure duration and determined the value of fluorescence change ($\Delta F/F$) by calculating $(F - F_0)/F_0$.

Photostimulation of TPH2-ChETA neurons in DR of DBA/1 mice mediated PTZ-induced S-IRA and c-fos expression in PBC

pAAV-TPH2 PRO-ChETA-EYFP-WPRES-PAS was delivered into the DR of DBA/1 mice 3 weeks before experiments, as previously described. The parameters for photostimulation of DR were: blue-light, 465 nm, 20 Hz, 20-ms pulse width, 15 mW, and 20 min. IP PTZ 15 min after photostimulation.

Immunohistochemistry and histology

The placement of the optical fiber cannula tip for ICV microinjection of KET within the bilateral PBC in each mouse was verified by histology. The PBC region was identified by neurokinin-1 receptor (NK1R) staining. DBA/1 mice were sacrificed and perfused with PBS (PBS) containing 4% paraformaldehyde (PFA). After

saturation in 30% sucrose (24 h), each mouse brain was sectioned into 30- μ m-thick coronal slices with a freezing microtome (CM30503, Leica Biosystems, Buffalo Grove, IL, USA). The sections were first washed in PBS three times for 5 min each and then incubated in blocking solution containing 10% normal donkey serum (017-000-121, Jackson ImmunoResearch, West Grove, PA, USA), 1% bovine serum albumen (A2153, Sigma-Aldrich), and 0.3% Triton X-100 in PBS for 1 h at room temperature. Then, for c-fos or TPH2 staining in the DR, sections were incubated at 4°C overnight in a solution of rabbit anti-c-fos primary antibody (1:1000 dilution, 2250 T Rabbit mAb/74,620 Mouse mAb, Cell Signaling Technology, Danvers, MA, USA) or mouse anti-TPH2 primary antibody (1:100 dilution, T0678, Sigma-Aldrich). The secondary antibodies used were donkey anti-mouse Alexa 488 (1:1000; A32766, Thermo Fisher Scientific, Waltham, MA, USA), donkey anti-mouse Alexa 546 (1:1000; A10036, Thermo Fisher Scientific), or goat anti-rabbit cy5 (1:1000; A10523, Thermo Fisher Scientific), and slices were incubated in secondary antibody solutions for 2 h at room temperature. Similarly, for neurokinin 1 receptor (NK1R) or SA-2A R (5-HT-2AR) staining in the PBC, sections were incubated in a solution of rabbit anti-NK1 (1:500 dilution, SAB4502913, Sigma-Aldrich) or mouse anti-SA-2A R (5-HT2AR) (1:100 dilution, sc-166775, Santa Cruz Biotechnology, Santa Cruz, CA, USA) at 4°C overnight followed by donkey anti-rabbit Alexa 488 secondary antibody (1:1000; A32766, Thermo Fisher Scientific), donkey anti-mouse Alexa 546 (1:1000; A10036, Thermo Fisher Scientific), or goat anti-mouse cy5 (1:400; A10524, Thermo Fisher Scientific) for 1 h at room temperature. After washing with PBS three times for 15 min each, the sections were mounted onto glass slides and incubated in DAPI (1:4000; Cat#C1002; Beyotime Biotechnology; Shanghai, China) for 7 min at room temperature. Finally, the glass slides were sealed using an anti-fluorescence attenuating tablet. All images were taken with a Nikon A1 laser-scanning confocal microscope (Nikon, Tokyo, Japan). The numbers of immunopositive cells were counted and analyzed using ImageJ (NIH, Bethesda, MD, USA). Notably, data from mice in which the implantation placement was outside of the targeted brain structure were not used in our experiments. Positively stained cells expressing c-fos, ChETA and TPH2 were counted as previously described (Zhao et al., 2019).

Viral vectors

pAAV-TPH2 PRO-ChETA-EYFP-WPRES-PAS (AVV2/8) (viral titer: 1×10^{13} vg/mL), was purchased from Sheng BO, Co., Ltd. (Shanghai, China), and the sequences of vectors were designed by Kazuki Nagayasu (Department of Molecular Pharmacology Graduate School of Pharmaceutical Sciences, Kyoto University). CTB-555 (1 μ g/ μ L) was purchased from Brain VTA Technology Co., Ltd. (Wuhan, China). AAV2/9-mCaMKIIa-GCaMP6f-WPRE-pA (viral titer: 1×10^{14} vg/mL) were purchased from Taitool Bioscience Co., Ltd. (Shanghai, China).

QUANTIFICATION AND STATISTICAL ANALYSIS

All data are presented as the mean \pm SEM. Statistical analyses were performed using SPSS 23 (SPSS Software Inc., Chicago, IL, USA). The incidence rates of S-IRA in different groups were compared using Wilcoxon signed rank test. Seizure scores, the latency to AGS_z, the duration of wild running and clonic seizures, and duration of tonic-clonic seizures were evaluated using one-way ANOVA, unpaired t test. One-way ANOVA test was used to compare the clonic seizures and tonic seizures peak $\Delta F/F$. two-way ANOVA test was used for EEG analysis. Unpaired t test was used to compare the numbers of c-fos-positive cells in the DR and PBC of DBA/1 mice with and without photostimulation. Statistical significance was inferred if $p < 0.05$. * $p < 0.05$, ** $p < 0.01$, *** $p < 0.001$ (Tables 1 and 2).

Summary of experimental groups of DBA/1 mice

Figure	Experimental groups	Number of mice
Figure 1	saline and 25% DMSO	7
	5-HTP and 25% DMSO	6
	5-HTP and KET (5 mg/kg)	6
	5-HTP and KET (10 mg/kg)	6
	5-HTP and KET (20 mg/kg)	6
	5-HTP and KET (25 mg/kg)	6
	5-HTP and KET (25 mg/kg)	11

(Continued on next page)

Continued		
Figure	Experimental groups	Number of mice
Figure 2	saline and 25 % DMSO	7
	5-HTP and 25% DMSO	7
	5-HTP and KET (9.15 nmol)	5
	5-HTP and KET (18.30nmol)	7
Figure 5/Figure 6	no photostimulation	7
	photostimulation	6
	photostimulation and KET	7
Figure 7	no photostimulation and 25 % DMSO(400 nL)	7
	photostimulation and 25% DMSO(400 nL)	7
	photostimulation and KET(400nL)	7
Figure 10	c-fos(+)/ChETA(+)/TPH2(+) cells	2
	with photostimulation	2
	without photostimulation	
Figure 11	no photostimulation	5
	photostimulation	6
	photostimulation and KET	3
Figure 12	no photostimulation	6
	photostimulation	6
Figure S1	25 % DMSO(400 nL)	7
	KET(400nL)	7
Figure S2	saline and 25 % DMSO	9
	5-HTP and 25% DMSO	8
	5-HTP and KET (400nL)	10
Figure S3	no photostimulation	7
	photostimulation	7
	quantification of c-fos(+)/5HT-2AR(+) cells	3

Statistical analysis		
Figure	Experimental groups	Number of mice
Figure 1	incidence of S-IRA	Wilcoxon signed-rank test
	latency to AGSz	Ordinary one-way ANOVA
	duration of wild running and clonic seizures	Ordinary one-way ANOVA
	duration of tonic-clonic seizures	Ordinary one-way ANOVA
	seizure scores	Ordinary one-way ANOVA
Figure 2	incidence of S-IRA	Wilcoxon signed-rank test
	GSz latency duration of wild running and clonic seizures	Ordinary one-way ANOVA
	duration of tonic-clonic seizures	Ordinary one-way ANOVA
	seizure scores	Ordinary one-way ANOVA
		Ordinary one-way ANOVA
Figure 5	incidence of S-IRA	Wilcoxon signed-rank test
	GSz latency duration of wild running and clonic seizures	Ordinary one-way ANOVA
	duration of tonic-clonic seizures	Ordinary one-way ANOVA
	seizure scores	Ordinary one-way ANOVA
		Ordinary one-way ANOVA
Figure 6	delta wave	two-way ANOVA
	theta wave	two-way ANOVA
	alpha wave	two-way ANOVA
	beta wave	two-way ANOVA
	gamma wave	two-way ANOVA

(Continued on next page)

Continued

Figure	Experimental groups	Number of mice
Figure 7	incidence of S-IRA GSz latency duration of wild running and clonic seizures duration of tonic-clonic seizures seizure scores	Wilcoxon signed-rank test Ordinary one-way ANOVA Ordinary one-way ANOVA Ordinary one-way ANOVA
Figure 10	quantification of c-fos(+)/ChETA(+)/TPH2(+) cells	Unpaired t test
Figure 11	incidence of S-IRA GSz latency duration of wild running and clonic seizures duration of tonic-clonic seizures seizure scores	Wilcoxon signed-rank test Ordinary one-way ANOVA Ordinary one-way ANOVA Ordinary one-way ANOVA Ordinary one-way ANOVA
Figure 12	clonic seizures of $\Delta F/F$ tonic seizures of $\Delta F/F$	Ordinary one-way ANOVA Ordinary one-way ANOVA
Figure S2	incidence of S-IRA GSz latency duration of wild running and clonic seizures duration of tonic-clonic seizures seizure scores	Wilcoxon signed-rank test Ordinary one-way ANOVA Ordinary one-way ANOVA Ordinary one-way ANOVA Ordinary one-way ANOVA
Figure S3	incidence of S-IRA GSz latency duration of wild running and clonic seizures duration of tonic-clonic seizures seizure scores quantification of c-fos(+)/5HT-2AR(+) cells	Wilcoxon signed-rank test Ordinary one-way ANOVA Ordinary one-way ANOVA Ordinary one-way ANOVA Ordinary one-way ANOVA Unpaired t test